Journal of Medicinal Chemistry

Article

Design, Synthesis, and Biological Evaluation of Novel Selenium-containing Isocombretastatins and Phenstatins as Antitumor Agents

Yanqing Pang, Baijiao An, Lanlan Lou, Junsheng Zhang, Jun Yan, Ling Huang, Xingshu Li, and Sheng Yin

J. Med. Chem., **Just Accepted Manuscript** • DOI: 10.1021/acs.jmedchem.7b00480 • Publication Date (Web): 09 Aug 2017

Design, Synthesis, and Biological Evaluation of Novel Selenium-containing *Iso*combretastatins and Phenstatins as Antitumor Agents

Yanqing Pang,† Baijiao An,† Lanlan Lou, Junsheng Zhang, Jun Yan, Ling Huang, Xingshu Li,* and Sheng Yin*

School of Pharmaceutical Sciences, Sun Yat-sen University, Guangzhou 510006, China

ABSTRACT: Two series of structurally-related organoselenium compounds designed by fusing the anticancer agent methyl(phenyl)selane into the tubulin polymerization inhibitors *iso*combretastatins or phenstatins were synthesized and evaluated for antiproliferative activity. Most of these selenium containing hybrids exhibited potent cytotoxicity against a panel of cancel cell lines, with IC_{50} values in the submicromolar concentration range. Among them, **11a**, the 3-methylseleno derivative of *iso*combretastatin A-4 (*iso*CA-4), represented the most active compound with IC_{50} values of 2−34 nM against twelve cancer cell lines, including two drug-resistant cell lines. Importantly, its phosphate salt, **11ab**, inhibited tumor growth in xenograft mice models with inhibitory rate of 72.9% without apparent toxicity, which was better than the reference compounds *iso*CA-4P (inhibitory rate: 52.2%) and CA-4P (inhibitory rate: 47.6%). Mechanistic studies revealed that **11a** is a potent tubulin polymerization inhibitor, which could arrest cell cycle at G_2/M phase and induce apoptosis along with the decrease of mitochondrial membrane potential. In summary, **11a** could serve as a promising lead for the development of highly efficient anticancer agents.

INTRODUCTION

The interfering with tubulin dynamics becomes a well-verified strategy for the development of highly efficient anticancer drugs because microtubules play a pivotal role in essential cellular processes including the movement of organelles, intracellular transportation, and the formation and maintenance of cell shape.[1] Natural products capable of interfering with the assembly or disassembly of microtubules have drawn much attention in the last decades, and a large number of natural tubulin modulators have been reported as anticancer agents. For instance, paclitaxel, currently used in the treatment of ovarian and breast cancer, could promote the polymerization of microtubules, resulting in highly stable, nonfunctional assembled microtubules,[2] while the vinca alkaloids (e.g. vincristine, vinblastine, etc.), dolastatins, and colchicine are well-known antitumor agents inhibiting microtubule assembly.[3] However, these complex molecules have limitations resulting from high toxicity, difficulty of synthesis, and some of them become rapidly prone to resistance phenomena.[4] Among the large class of natural tubulin polymerization inhibitors, combretastatin A-4 (CA-4), isolated from the African willow tree *Combretum caffrum*, represents currently the simplest structure and its soluble prodrug, CA-4P, has been approved as orphan drug for the treatment of anaplastic thyroid cancer by both the FDA and European Medicines Agency.[5, 6] However, the *Z*-natural stilbene compound is prone to double-bond isomerization during storage and administration, leading to the *E*-isomer, which displayed a dramatically reduced activity.[7] Thus, the drug discovery campaign based on the rational design of CA-4 derivatives has been

extensively carried out in the last few decades, which led to the synthesis of more than 28000 analogues.[8] Among them, *iso*combretastatin A-4 (*iso*CA-4), a 1,1-diarylethylene isomer of CA-4, and phenstatin, a ketone bioisostere of *iso*CA-4, turned out to be the most promising antitubulin agents with comparable in vitro activity to that of CA-4,[9] although the in vivo antitumor effects of these compounds have not been investigated yet.

Selenium (Se) compounds have attracted a vast interest recently as promising chemo-preventive agents, and several organoselenium compounds have been shown to inhibit cancer cell growth in various xenograft rodent models for different cancers types, as well as to have synergistic effects in combination with chemotherapeutic drugs.[10, 11] Among them, the arylselenium compounds, such as methyl(phenyl)selane,[10] benzeneselenol,[12] and methylselenocysteine[11] represent a group of simple but well-studied anticancer molecules, which exert their antitumor effects by induction of apoptosis, inhibition of angiogenesis, and modulation of AKT and COX pathways.[11, 13]

Despite the impressive number of CA-4 analogues have been reported, only a few CA-4 analogues containing selenium atoms as spacer groups between the aromatic rings (diaryl selenide,[14] 3,4-diaryl-1,2,5-selenadiazol,[15] and selenoxides[16]) have been studied. However, these compounds only exhibited similar antiproliferative activity to CA-4 in vitro, without any further evaluation in vivo, and the introduction of selenium atoms on the aromatic rings has never been studied. Considering all of the above-mentioned information, we hypothesized that assembly of *iso*combretastatins

or phenstatins with methyl(phenyl)selane in the same molecule could be a valid shortcut in the development of new anticancer agents.

To fuse these two scaffolds, there are three potential sites that can be modified (C-3, C-4 and C-4'). Firstly, we have tried to introduce a selenium atom on C-4 position of A-ring, but the reaction hardly took place because of the stereo-hindrance of two *ortho*-positioned methoxy groups. Then, the introduction of a selenium atom on C-4' position of B-ring was conducted. However, the the cytotoxicity of the resulting derivatives did not show too much improvements (see Table 1). Thus, the modification was conducted on the C-3 of ring A, and two series of structurally-related selenium-containing molecules were designed, synthesized, and evaluated for their antitumor potential in the current study.

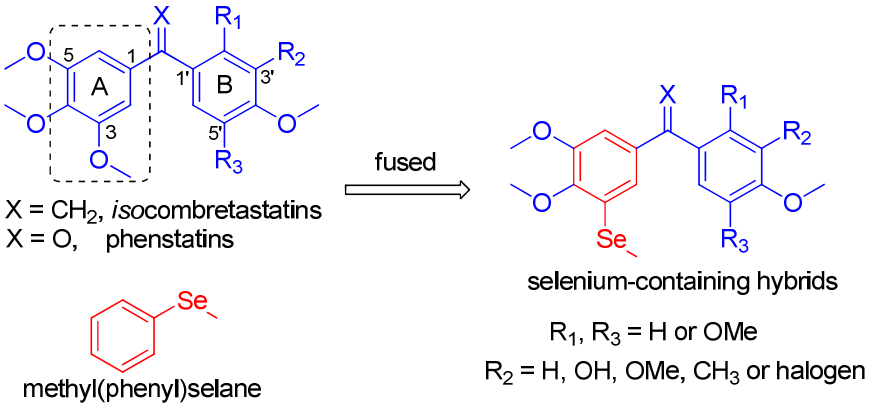

Figure 1. Design strategy of selenium-containing *iso*combretastatins and phenstatins

RESULTS AND DISCUSSION

Chemistry. The synthetic route of the selenium-phenstatin hybrids **10a–i** was summarized in Scheme 1. The reaction of 2-methoxyphenol **1** with NBS in the solution of acetonitrile provided 4-bromo-2-methoxyphenol **2**, and then, the nitration

of **2** gave intermediate **3**,[17] which reacted with methyl iodide to produce 5-bromo-1,2-dimethoxy-3-nitrobenzene **4**. The reduction of **4** with iron powder afforded the amino intermediate **5**,[18] which was diazotized by the hydrochloric acid and sodium nitrite, then followed by reaction with potassium selenocyanante to produce **6**. In the presence of potassium hydroxide in methanol, **6** was converted to diselenide **7**, which reacted with sodium borohydride and methyl iodide to afford the key intermediate **8**.[19] The reaction of **8** with different benzaldehyde analogues afforded diarylmethanols **9a–i**.[20] Finally, target compounds **10a–i** were obtained by the oxidation of **9a–i** with 2-iodoxybenzoic acid in good yields.[21]

Scheme 1. Synthesis of compounds **10a–i**[a]

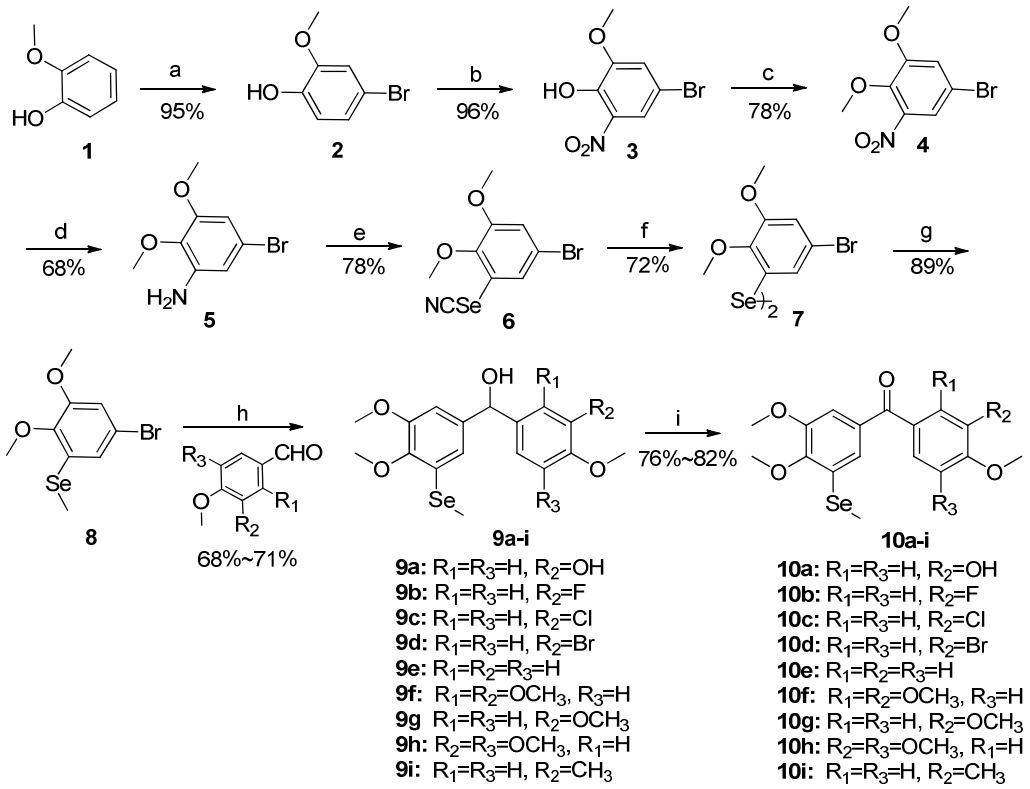

[a]Reagents and reaction conditions: (a) NBS, CH_3CN; (b) 65% HNO_3, AcOH; (C) CH_3I, KOH, TBAI, DMF; (d) iron powder, AcOH, EtOH; (e) $NaNO_2$, 10% HCl, KSeCN; (f) KOH, CH_3OH; (g) $NaBH_4$, CH_3I, EtOH; (h) *n*-BuLi, anhydrous THF; (i) IBX, THF.

The selenium-*iso*CA hybrids **11a–i** were synthesized commodiously by employing Wittig reactions between **10a–i** and methyltriphenylphosphonium bromide (Scheme 2).[9]

Scheme 2. Synthesis of compounds **11a–i**[a]

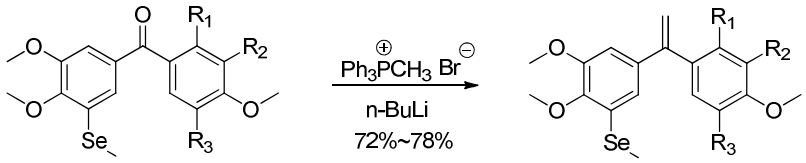

10a-i
10a: R_1=R_3=H, R_2=OH
10b: R_1=R_3=H, R_2=F
10c: R_1=R_3=H, R_2=Cl
10d: R_1=R_3=H, R_2=Br
10e: R_1=R_2=R_3=H
10f: R_1=R_2=OCH_3, R_3=H
10g: R_1=R_3=H, R_2=OCH_3
10h: R_2=R_3=OCH_3, R_1=H
10i: R_1=R_3=H, R_2=CH_3

11a-i
11a: R_1=R_3=H, R_2=OH
11b: R_1=R_3=H, R_2=F
11c: R_1=R_3=H, R_2=Cl
11d: R_1=R_3=H, R_2=Br
11e: R_1=R_2=R_3=H
11f: R_1=R_2=OCH_3, R_3=H
11g R_1=R_3=H, R_2=OCH_3
11h: R_2=R_3=OCH_3, R_1=H
11i: R_1=R_3=H, R_2=CH_3

[a]Reagents and reaction conditions: Methyltriphenylphosphonium bromide, n-BuLi, anhydrous THF.

To investigate the effect of different substituting position of selenium on the activity, compounds **17** and **18** with the selenium atom on the C-4′ position of the B-ring were synthesized using the same procedures as those of **10a–i** and **11a–i** apart from the use of 4-bromoaniline (**12**) as the starting materials (Scheme 3).

Scheme 3. Synthesis of compounds **17** and **18**[a]

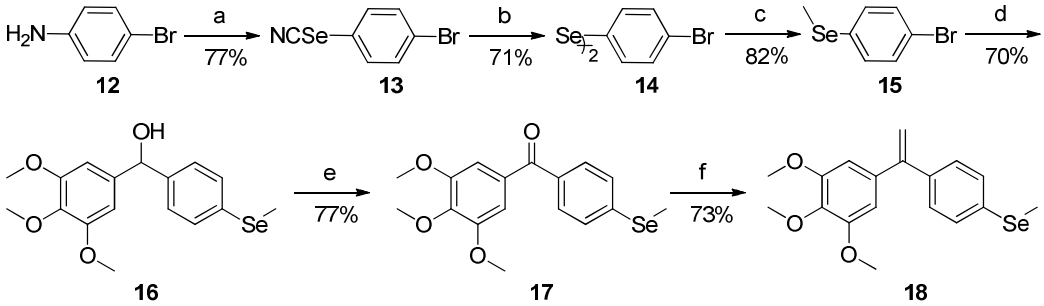

[a]Reagents and reaction conditions: (a) $NaNO_2$, 10% HCl, KSeCN; (b) KOH, CH_3OH; (c) $NaBH_4$, CH_3I, EtOH; (d) *n*-BuLi, anhydrous THF; (e) IBX, THF.(f) methyltriphenylphosphonium bromide, n-BuLi, anhydrous THF.

Considering the bioavailability of drugs largely depends on their water solubility, **11ab**, the disodium phosphate salt of **11a**, was synthesized for the in vivo test. As shown in Scheme 4, the esterification reaction between **11a** and diethyl phosphite afforded **11aa**, which was deprotected in trimethylsilyl bromide then followed by neutralization with NaOH to give the target compound **11ab**.

Scheme 4. Synthesis of compound **11ab**[a]

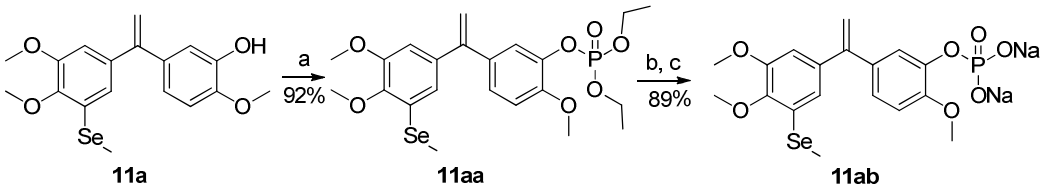

[a]Reagents and reaction conditions: (a) diethyl phosphite, Et_3N, CCl_4, CH_2Cl_2; (b) TMSBr, anhydrous CH_2Cl_2; (c) NaOH, MeOH.

BIOLOGY

Antiproliferative Activities and the SARs. To evaluate the synergistic effects of these selenium-containing hybrids, benzophenone derivative **10a**, bearing a methylselanyl to replace the 3-methoxyl of phenstatin, was first synthesized and screened for antiproliferative activity against a panel of five different cancer cell lines [A549 (human non-small cell lung carcinoma), MDAMB231 (human breast carcinoma), HEPG2 (human hepatoma carcinoma), LOVO and RKO (human colorectal carcinoma)]. As shown in Table 1, **10a** exhibited pronounced activity with IC_{50} values ranging from 24 to 79 nM, being more potent than the prototype compound phenstatin. In order to investigate the structures-activity relationships of these selenium-phenstatin hybrids, compounds **10b–10i** with different substituents at C-2′, C-3′, and C-5′ of ring B (R_1, R_2, and R_3) were prepared and evaluated for their

antiproliferative activities. Compound **10b** with the presence of a fluorine atom at C-3′ (R_2 = F), displayed similar activity to those of **10a** (R_2 = OH) and **10e** (R_2 = H), with IC_{50} values ranging from 33 to 59 nM. When fluorine atom was replaced by chlorine or bromine atom, the activities decreased dramatically as shown in **10c** (R_2 = Cl, IC_{50} = 253 ~ 1534 nM) and **10d** (R_2 = Br, IC_{50} = 169 ~ 1752 nM). These results suggested that the large hetero atoms at C-3′ might be adverse to the activity. Compounds **10f–10h** provide less potent activity than those of **10a** or **10e**, indicating that the excess of methoxy groups at B ring was unfavorable to the activity, especially the presence of methoxy group at C-3′ (R_2 = OMe). Similarly, the presence of methyl at C-3′ (R_2 = Me) also led to the dramatically decrease of the activity, as **10i** only provided a poor activity with IC_{50} values ranging from 997 to 5281 nM.

Inspired by above results, selenium-*iso*CA hybrids **11a–i** were synthesized and evaluated. As shown in Table 1, It is interesting that the replacement of the carbonyl group with a terminal double bond led to the different effect on the activity, as the increased activity (**11a** vs **10a**, **11c** vs **10c**, and **11i** vs **10i**) and decreased activity (**10h** vs **11h**) were both observed in these pairs of compounds. Within **11a–i**, similar SARs were observed as selenium-phenstatin series and **11a** turned out to be the most active compound with the IC_{50} values of 2.2−11 nM toward five cancer cell lines.

Compounds **17** and **18** with the selenium atom on the C-4′ position also exhibited pronounced activity (**17**, IC_{50}: 66 ~ 296 nM; **18**, IC_{50}: 97 ~ 386 nM). However, comparing with their C-3 selenium counterparts **10e** and **11e**, the generally weaker activities of **17** and **18** indicated that the substitution of selenium on C-3 is beneficial.

Table 1. Antiproliferative Activities of **10a–i** and **11a–i** against Human Cancer Cell Lines[a]

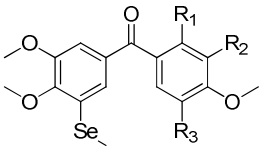

10a: R_1=R_3=H, R_2=OH
10b: R_1=R_3=H, R_2=F
10c: R_1=R_3=H, R_2=Cl
10d: R_1=R_3=H, R_2=Br
10e: R_1=R_2=R_3=H
10f: R_1=R_2=OCH_3, R_3=H
10g: R_1=R_3=H, R_2=OCH_3
10h: R_2=R_3=OCH_3, R_1=H
10i: R_1=R_3=H, R_2=CH_3

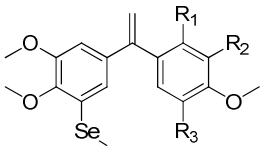

11a: R_1=R_3=H, R_2=OH
11b: R_1=R_3=H, R_2=F
11c: R_1=R_3=H, R_2=Cl
11d: R_1=R_3=H, R_2=Br
11e: R_1=R_2=R_3=H
11f: R_1=R_2=OCH_3, R_3=H
11g R_1=R_3=H, R_2=OCH_3
11h: R_2=R_3=OCH_3, R_1=H
11i: R_1=R_3=H, R_2=CH_3

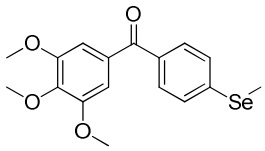

17

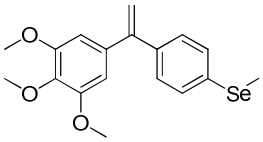

18

Compd	IC_{50} (nM)[b]				
	A549	MDAMB231	HEPG2	LOVO	RKO
10a	55 ± 4	24 ± 7	31 ± 4	53 ± 14	79 ± 18
10b	33 ± 8	34 ± 8	47 ± 11	57 ± 9	59 ± 6
10c	949 ±12	865 ± 14	1534 ± 290	189 ± 15	253 ± 70
10d	368 ± 36	435 ± 15	655 ± 98	1752 ± 93	169 ± 15
10e	31 ± 8	57 ± 5	85 ± 9	145 ± 14	47 ± 7
10f	2746 ± 200	4257 ± 400	4338 ± 220	523 ± 28	874 ± 60
10g	285 ± 52	1016 ± 130	1086 ± 130	766 ± 10	306 ± 30
10h	172 ± 12	741 ± 74	288 ± 29	921 ± 38	235 ± 60
10i	1728 ± 15	997 ± 80	2296 ± 220	3150 ± 340	5281 ± 510
11a	3.9 ± 1	2.2 ± 1	3 ± 1	9 ± 3	11 ± 5
11b	29 ± 3	24 ± 3	87 ± 5	33 ± 3	82 ± 9
11c	196 ± 20	83 ± 8	298 ± 60	254 ± 30	451 ± 53
11d	236 ± 15	667 ± 100	691 ± 50	171 ± 16	343 ± 75
11e	72 ± 22	96 ± 23	126 ± 70	91 ± 9	107 ± 14
11f	1380 ± 150	3825 ± 780	6299 ± 750	128 ± 18	1036 ± 250
11g	265 ± 70	344 ± 80	473 ± 51	299 ± 152	216 ± 49
11h	473 ± 9	3324 ± 150	1350 ± 260	3145 ± 510	3516 ± 310
11i	141 ± 35	599 ± 47	607 ± 61	496 ± 55	245 ± 26
17	69 ± 2	65 ± 3	77 ± 2	296 ± 18	66 ± 3
18	97 ± 2	178 ± 6	386 ± 33	279 ± 6	216 ± 23
phenstatin	179 ± 30	62 ± 6	108 ± 4	122 ± 50	72 ± 18
*Iso*CA-4	3.5 ± 1	8.5 ± 2	18.3 ± 3	3.7 ± 2	3.8 ± 1
CA-4	4 ± 1[c]	4.1 ± 2[c]	3.9 ± 1[c]	2.4 ± 1	9.8 ± 2

[a]Cell lines were treated with compounds for 48 h. Cell viability was measured by MTT assay as described in the Experimental Section. [b]IC_{50} values are indicated as the mean ± SD (standard error) of at least three independent experiments. [c]Values were also reported as 9 ± 2, 3, and 2.1 ± 0.5 nM in literatures 22, 9a, and 23, respectively.

11a Inhibits another Five Human Cancer Cell Lines. As the most potent compound found in the initial cytotoxicity screening, **11a** was selected for further evaluation against another five different cancer cell lines [MCF7 (human breast carcinoma), HELA (human cervical carcinoma), HCT116 (human colon carcinoma), MGC803 (human gastric adenocarcinoma), and A2780 (human ovarian carcinoma)]. As shown in Table 2, **11a** also exhibited excellent antiproliferative activity with IC_{50} values in the low nanomolar range (IC_{50} = 3 ~ 27 nM). All these data suggested that **11a** was a potential anticancer agent worthy of further study.

Table 2. Antiproliferative Activities of **11a** on another Five Human Cancer Cell Lines[a]

Compd	IC_{50} (nM)[b]				
	MCF7	HELA	HCT116	MGC803	A2780
11a	27 ± 6	3 ± 0.2	12 ± 0.2	9± 0.4	6 ± 0.1
*Iso*CA-4	48 ± 0.9	6 ± 0.1	24 ± 0.5	19.8 ± 0.2	26 ± 0.6
CA-4	14 ± 0.5	3.8 ± 0.2	7 ± 0.1	8.9 ± 0.1	12 ± 0.3

[a]Cell lines were treated with compounds for 48 h. Cell viability was measured by MTT assay as described in the Experimental Section. [b]IC_{50} values are indicated as the mean ± SD (standard error) of at least three independent experiments.

Antiproliferative Activity of 11a against Drug-Resistant Cancer Cell Lines. Multidrug resistance (MDR) is a major obstacle for successful treatment of cancer, as rapidly acquired drug resistance often results in clinical chemotherapy failure. To evaluate the anti-MDR potential of **11a**, the cisplatin-resistant cell line A549/CDDP and the doxorubicin-resistant cell line HEPG2/DOX were selected for antiproliferative study. As shown in Table 3, **11a** inhibited A549/CDDP and HEGP2/DOX with IC_{50} values being at 34.4 and 20.3 nM, respectively. The small resistant factor values (RF: 8.8 and 6.8, respectively) suggested that **11a** possessed

potent antiproliferative activities towards drug-resistant cancer cell lines, which deserves further study.

Table 3. Antiproliferative Activities of **11a** towards Human Drug-Resistant Cancer Cell Lines[a]

compd	IC_{50} (nM)[b]					
	A549/CDDP	A549	Resistant factor[b]	HEPG2/DOX	HEPG2	Resistant factor[b]
11a	34.4 ± 0.9	3.9 ± 1	8.8	20.3 ± 0.6	3 ± 1	6.8
*Iso*CA-4	69.1 ± 0.4	3.5 ± 0.1	19.7	38.6 ± 0.2	18.3 ± 0.3	2.1

[a]Data are presented as the mean ± SE from the dose-response cures of at least three independent experiments.

[b]Resistant factor = (human drug-resistance cells IC_{50}) / (human cancer sensitive cells IC_{50}).

11a Inhibits Microtubule Polymerization. To elucidate whether **11a** targets the tubulin-microtubule system, the in vitro tubulin polymerization inhibition activity of **11a** was evaluated by using the method originally described by D. Bonne et al. with some modifications.[24, 25] As shown in Figure 2, the increased fluorescence intensity with time of the purified and unpolymerized tubulin control samples indicated that tubulin polymerization had occurred. After tubulin was incubated with **11a** at various concentrations ranging from 0.3125 to 7.5 μM, the increased tendency of the fluorescence intensity was obviously slowed down as compared with the control, indicating that **11a** inhibited the tubulin polymerization. Additionally, the results also indicated that **11a** inhibited tubulin polymerization in a dose-dependent manner, with an IC_{50} value of 1.38 ± 0.09 μM (Figure 2A), being stronger than the reference compound *iso*CA-4 (IC_{50} = 2.76 ± 0.11 μM, Figure 2B).

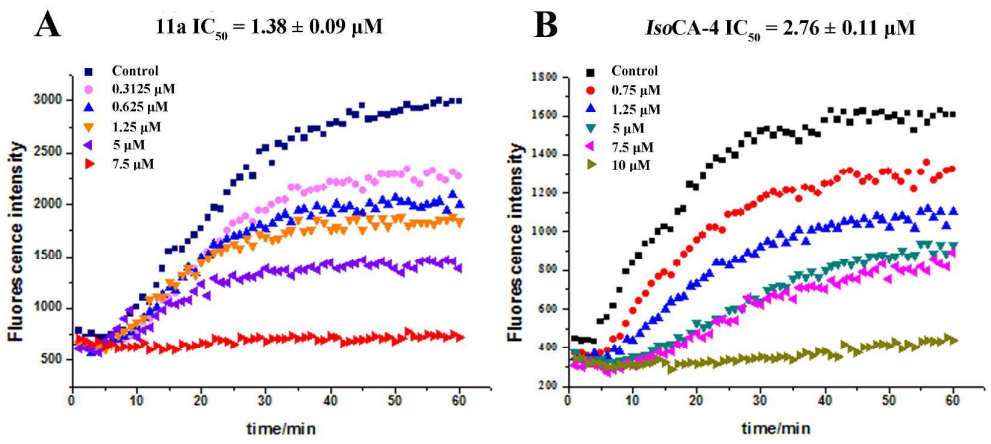

Figure 2. Compound **11a** inhibits microtubule polymerization. Purified tubulin protein at 10 mM in a reaction buffer was incubated at 37℃ in the absence (control) or presence of **11a** (A) and *iso*CA-4 (B) at the indicated concentrations (ranging from 0.3125 to 7.5 μM and 0.75 to 10 μM, respectively). The experiments were performed three times, and the results of representative experiments are shown.The IC_{50} value of *iso*CA-4 was also reported as 2.2 μM in literature 9a.

To study whether **11a** could disrupt the microtubule dynamics in living cells, immunofluorescence assay in A549 cells were performed, and *iso*CA-4 was used as the reference compound. As shown in Figure 3, in the control group, the microtubule network in the A549 cells exhibited normal arrangement and organization, characterized by regularly assembled, normal filiform microtubules wrapped around the uncondensed cell nucleus. After exposure to **11a** for 8 h, the spindle formation demonstrated distinct abnormalities and was heavily disrupted. Especially, when the concentration of **11a** was increased to 10 nM, the microtubule spindles wrapped around the cell nucleus have significantly shrunk and a number of dotted disorder formations were easily observed (Figure 3A). In contrast, cells treated with 10 nM of *iso*CA-4 for 8 h still retained a spindle shaped microtubule network but showed slight

changes on the shape of the nucleus (Figure 3B). When the incubation time was extended to 24 h, the multipolarization of the spindle and multinucleation phenomena were found in both groups treated with 10 nM samples. These morphological microtubule changes indicated that **11a** dramatically disrupted the microtubule organization at nanomolar concentrations, which might eventually lead to cell cycle disorder.

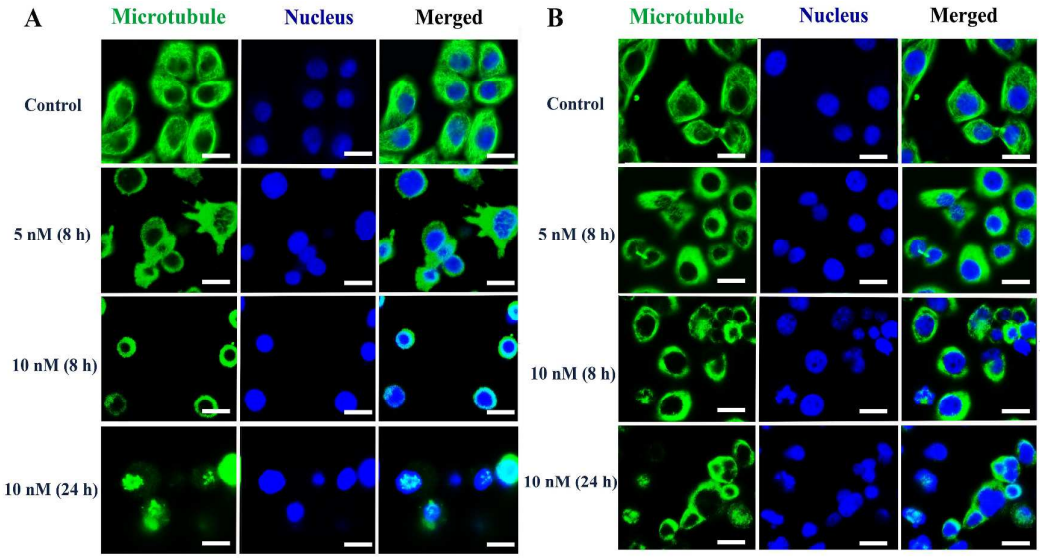

Figure 3. Compound **11a** (A) and *iso*CA-4 (B) disrupted the organization of the cellular microtubule network at indicated concentrations. A549 cells were plated in confocal dishes and incubated with DMSO or **11a** at the 5, 10 nM for 8 h and 24 h, followed by direct microscopy. The detection of the fixed and stained cells was performed with an LSM 570 laser confocal microscope (Carl Zeiss, Germany). The experiments were performed three times, and the results of the representative experiments were shown. Scale bar: 20 μm.

11a Induces Mitochondrial Dysfunction. A prelusion of cell apoptosis was the mitochondrial membrane depolarization, which usually leads to the decrease of

mitochondrial membrane potential (MMP, ΔΨm).[26] The change of MMP could be detected by flow cytometry analysis or a fluorescence microscope. To explore whether **11a** could induce mitochondrial dysfunction, quantitative mitochondrial membrane potentials (MMPs) assay of JC-1 staining mitochondria in A549 cells was performed. As shown in Figure 4A, the cells of control group have well-defined integral mitochondrial membranes (monomers: aggregates = 0.62 : 99.18), and after cells exposed to 1 nM of **11a**, the red fluorescence intensity (JC-1 aggregates, cells with high mitochondrial membrane potentials) decreased to 86.88%, and the green fluorescence intensity (JC-1 monomers, low mitochondrial membrane potentials) correspondingly increased from 0.62% to 12.78%. When increasing the concentration of **11a** to 5 nM and 10 nM, the red fluorescence intensity decreased to 57.63% and 9.14%, respectively, and the green fluorescence intensity correspondingly increased to 42.63% and 90.78%. These phenomena were also verified by the fluorescence microscopy assay, in which the treatment of **11a** induced the increase of the monomers and the decrease of the aggregates (Figure 4B). Taken together, **11a** could induce MMP collapse and mitochondrial dysfunction, which eventually triggers apoptotic cell death.

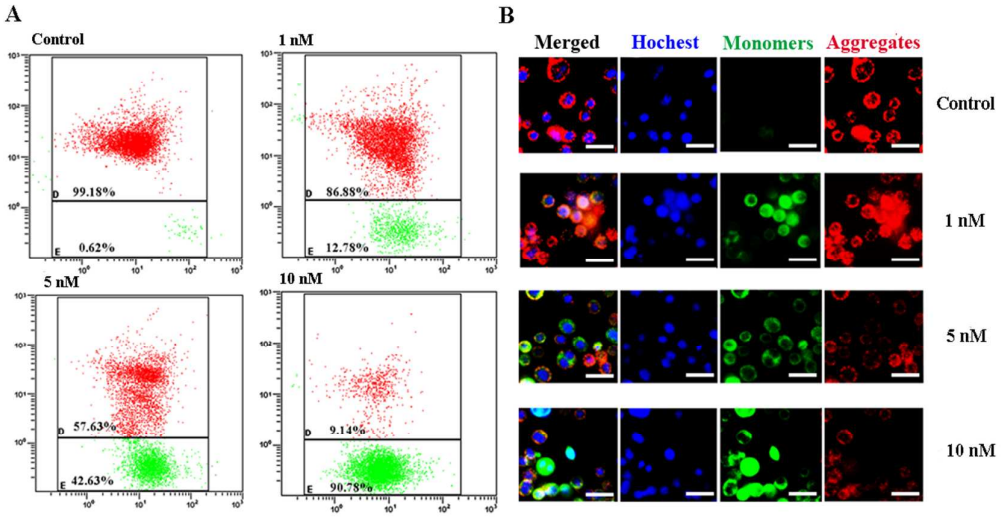

Figure 4. Compound **11a** decreased the mitochondrial membrane potential in a dose-dependent manner. The A549 cells were treated with **11a** at the indicated concentration (1, 5, and 10 nM) or DMSO (0.01%) for 24 h, followed by incubation with the fluorescence probe JC-1 for 30 min. Then, the cells were analyzed by flow cytometry (A) or fluorescence microscope (B). The experiments were performed at least three times, and the results of the representative experiments. Scale bar: 20 μm.

11a Induces G_2/M Phase Arrest and Regulates the Expression of G_2/M-Related Proteins. As most tubulin destabilizing agents could disrupt the regulated cell cycle distribution, a flow cytometry analysis was performed to determine the arrest effect of **11a** on the G_2/M transition, a rigorously regulated process in the cell cycle. As shown in Figure 5, **11a** effectively arrested cells in the G_2/M phase in a dose- and time-dependent manner. When A549 cells were treated with **11a** from 1 nM to 10 nM for 12 h, the population of cells in G_2/M phase dramatically increased as compared to that of vehicle (DMSO) group (Figure 5A), along with concomitant losses in the G_1 phase. This phenomenon was more obvious after 24 h incubation, when nearly 50% cells were arrested at G_2/M phase at the concentration of 1 nM, and about 70% cells

were arrested at concentrations of 5 nM or 10 nM. It is known that the activation of Cdc2 kinase controlled by Cyclinb1 binding and Cdc25C phosphorylation could regulate eukaryotic cell entry into mitosis, leading to the cell division.[27, 28] Thus, the association between **11a**-induced G_2/M arrest and the alterations of these protein expression were investigated by western blot analysis. As shown in Figure 5C, after A549 cells were treated with **11a** at the concentrations of 1, 5, and 10 nM for 12h, the expression of Cdc25C, Cdc2 and Cyclinb1 protein distinctly decreased in dose- and time-dependent manners. The phenomenon was more obvious when the treatment time was extended to 24 h. These results, which were consistent with the cell cycle analysis and the intracellular microtubule immunofluorescence assay, further illustrated the basic mechanism of **11a** on the cell cycle arrest.

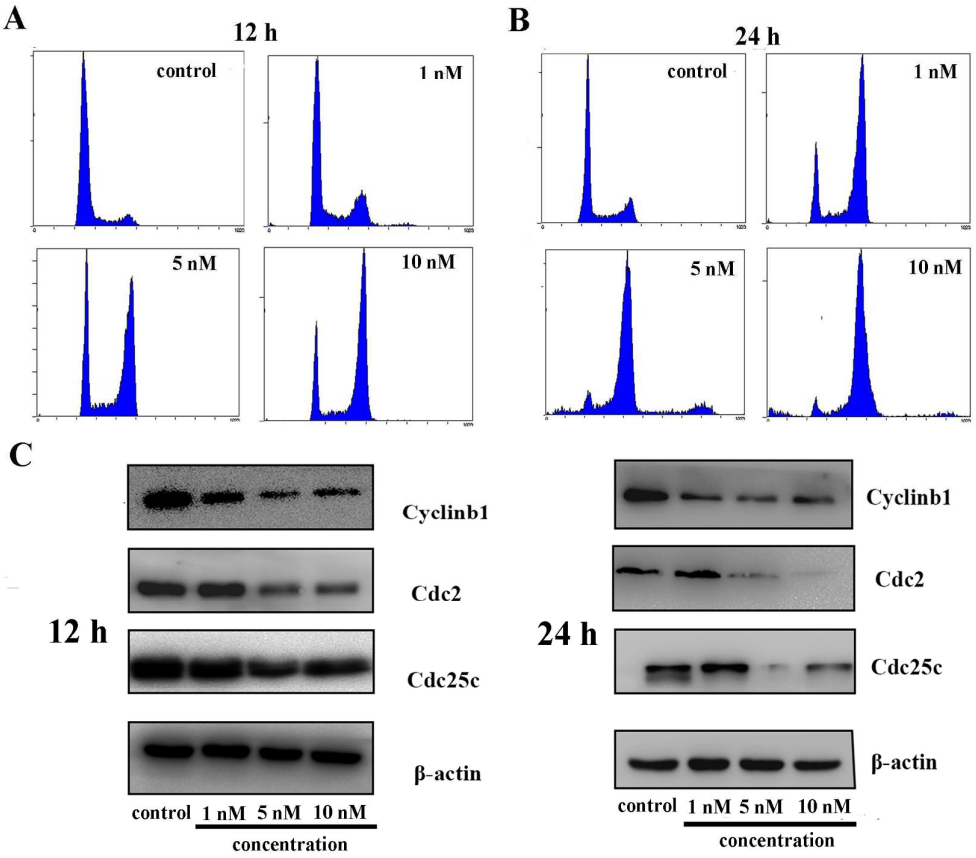

Figure 5. Cell cycle arrest effect of **11a**. The A549 cells were treated with compound **11a** at 1, 5, or 10 nM for 12 h (A) or 24 h (B). The expression of proteins Cyclin B1, Cdc25c, and Cdc2 were analysed by the western blot (C). The experiments were performed three times, and the results of representative experiments are shown.

11a Induces Apoptosis via the Regulation of Apoptosis-Related Proteins Expression. According to above-mentioned cell cycle analysis, we suppose that **11a** might induce the apoptosis of A549 cells. To confirm this, A549 cells were treated with 1 nM to 10 nM of **11a** for 24 h or 48h, and then, the cells was harvested and stained with Annexin V-FITC and propidium iodide (PI), and analyzed by flow cytometry. As shown in Figure 6A, when the cells were incubated with **11a** at 1, 5, and 10 nM for 24 h, the percentages of early and late apoptosis cells were 3.64%, 33.88%, and 50.93%, respectively, being elevated from the control group (0.82%). After 48 h incubation at 1, 5, and 10 nM, the percentages of early and late apoptotic cells were strikingly increased to 18.65%, 40.42%, and 63.01%, respectively (Figure 6B). The Bcl-2 family proteins are critical regulators of cell apoptosis,[29] which can either promote the release of cytochrome c and further induce cell apoptosis (e.g. Bax, Bid, Bim, and Bad), or antagonize the pro-apoptotic proteins to prevent apoptosis (e.g. Bcl-2, Bcl-xl, and Bcl-w).[30, 31] To determine the apoptosis-associated protein alterations, the expression of Bad, Bcl-2, and Bcl-xl were analyzed. As shown in Figure 6D, when A549 cells were treated with **11a** at different concentrations (1, 5, and 10 nM) for 24 h or 48 h, the level of Bad was efficiently up-regulated, whereas the level of anti-apoptotic proteins (Bcl-2, Bcl-xl) was down-regulated significantly.

These results demonstrated that **11a** induced the cell cycle arrest and eventually led to cell apoptosis.

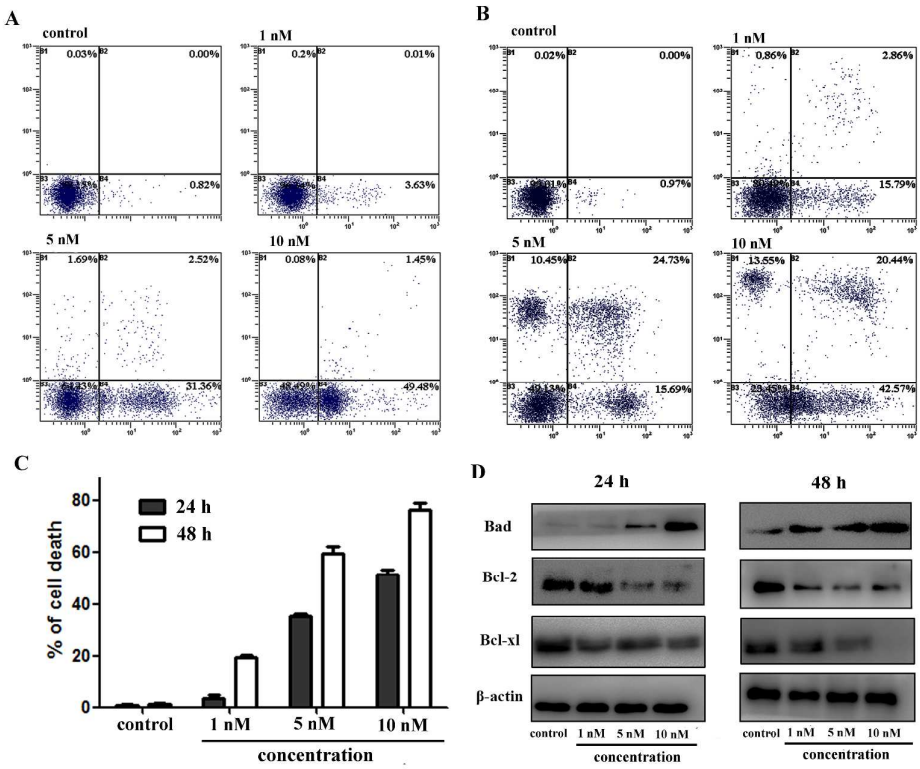

Figure 6. Compound **11a** induced A549 cell apoptosis. The A549 cells were treated with compound **11a** at 1, 5, or 10 nM for 24 h (A) or 48 h (B). The percentages of cells in each stage of cell apoptosis were quantified by flow cytometry: (upper left quadrant) necrosis cells; (upper right quadrant) late-apoptotic cells;(bottom left quadrant) live cells; and (bottom right quadrant) early apoptotic cells, total apoptosis cells percentage were obtained by EXPO32 ADC analysis software (C) And anlysed the expression of proteins Bad, Bcl-2, and Bcl-xl by the western blot (D). The experiments were performed three times, and the results of representative experiments are shown.

Metabolic Stability of 11a. To provide some basic information of drug-like properties, the metabolic stability of **11a** with rat liver microsomes was performed, and CA-4 and *iso*CA-4 were used as the reference compounds.[32] These compounds were incubated with rat liver microsomes in vitro at 37 °C for an indicated time in

buffer solution containing NADPH regenerating system, and the residues were determined by HPLC. As shown in Table 4, the remaining percentage of **11a** at each time point was higher than that of CA-4 but lower than that of *iso*CA-4. After 150 min incubation while **11a** and *iso*CA-4 still remained 25.8% and 34.3%, respectively, CA-4 couldn't be detected. A short half-life of pharmaceutical agents might result in low bioavailability in vivo and the frequent administration with a high dose, which might cause the drug accumulation and produce related toxicity. The half-lives of **11a** ($t_{1/2}$ = 74.5 min), *iso*CA-4 ($t_{1/2}$ = 101.9 min), and CA-4 ($t_{1/2}$ < 60 min) indicated that **11a** possessed a comparable metabolic stability to that of *iso*CA-4, being greater than CA-4, which encouraged us to carry out further studies in vivo.

Table 4. Metabolic Stability of **11a,** CA-4, and *iso*CA-4.

Compd	Time (min)	Remains %					
		30	60	90	120	150	$t_{1/2}$
11a		81.1%	62.3%	44.1%	33.4%	25.8%	74.5
CA-4		67.2%	26.4%	22.5%	19.9%	NT[a]	ND[b]
*Iso*CA-4		85.7%	77.1%	67.3%	49.8%	34.3%	101.9

[a]NT: not tested because of the fast metabolic rate of CA-4. [b]ND: not determined.

Antitumor Effect of 11ab in vivo. To determine the in vivo antitumor effect of **11a**, nude mouse A549 xenograft models were established by subcutaneously injecting A549 cells in the logarithmic phase into the right armpit of the mice. Considering the bioavailability of drugs largely depends on their water solubility, **11ab**, the disodium phosphate salt of **11a** was synthesized as the prodrug for the in vivo test. The mice were randomly allocated to four groups with nine of each (vehicle-treated, CA-4P-treated, *iso*CA-4P-treated, and **11ab**-treated groups). After the tumor volume was 100-200 mm^3 in each group, **11ab**, CA-4P, and *iso*CA-4P were intraperitoneally

injected at a dose of 30 mg/kg to the mice every other day for the entire observation period. As showed in Figure 7, at the end of the observation period, **11ab**, CA-4P, and *iso*CA-4P groups gave 467.21, 926.50 and 829.79 mm^3 of the mean final tumor volume, respectively, comparing the 1775.45 mm^3 of the vehicle group. The average tumor weight of the **11ab**-treated group was 0.432 g (inhibitory rate: 72.9%) comparing with 1.595 g of the vehicle group, which was less than that of CA-4P-treated group (0.835 g, inhibitory rate: 47.6%) and *iso*CA-4P-treated group (0.765 g, inhibitory rate: 52.2%). It also can be seen from Figure 7E that all the groups gave nearly the same body weights, indicating the low toxicity of **11ab** toward mice.

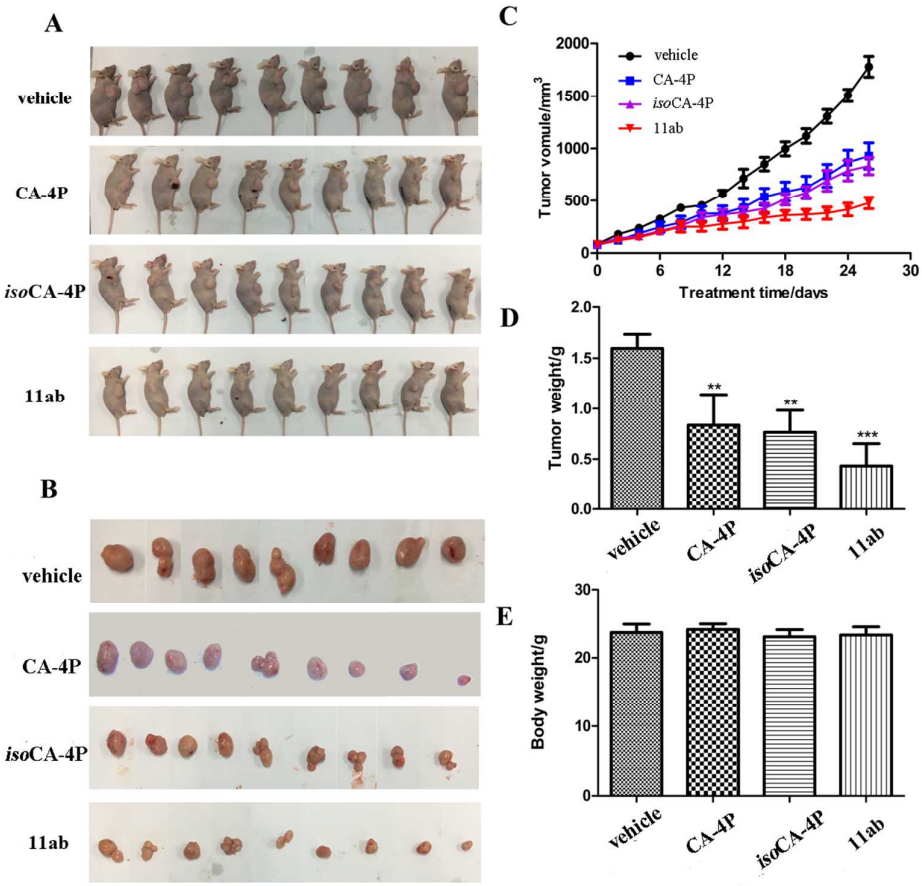

Figure 7. Efficacy of **11ab** against A549 xenografts. (A, B) The images of sacrificed mice and excised tumours in each group. (C) The tumour volume of mice in each group during observation period. (D) The weight of the excised tumors in each group. (E) The body weight of the mice in each group at the end of the observation period. The data were presented as the mean ± SEM *P < 0.05, **P < 0.01, ***P < 0.001, significantly different compared with the control by *t* test, n = 9. Data were not in conformity with Mauchly's test of sphericity, and Greenhouse−Geisser was performed to correction.

CONCLUSIONS

The multifactorial mechanistic characteristics of cancer results the possibility of incorporating a sequential, multifactorial approach to the multifaceted disease. Inspired by this, in the current study, two series of structurally-related organoselenium compounds were obtained by fusing the anticancer agent methyl(phenyl)selane into the tubulin polymerization inhibitors *iso*combretastatins and phenstatins, respectively. Most of these compounds exhibited potent antiproliferative activity against five human cancer cell lines, with IC_{50} values in the submicromolar concentration range. Among them, the optimal compound **11a** displayed excellent activities in twelve human cancer cell lines, including two drug-resistant cancer cell lines. Importantly, its phosphate salt, **11ab** exhibited obviously synergistic antitumor effects in A549 xenograft model in vivo without apparent toxicity, being better than the reference compound *iso*CA-4P. In addition, the in vivo antitumor effect of *iso*CA-4P was investigated for the first time. Finally, the mechanistic studies including the action of **11a** on tubulin polymerization, cell-cycle arrest, cell apoptosis effect, mitochondrial

dysfunction and the morphological alterations of A549 cell were also performed. All of these results demonstrated that the introduction of selenium atom at the C-3 of *iso*CA-4 elevated its anticancer effect, probably by mediating on several mechanisms, which make **11a** a promising lead for further anticancer-drug development.

EXPERIMENT SECTION

Chemistry. General Methods. Reagents used in the synthesis were obtained commercially and used without further purification, unless otherwise specified. Flash column chromatography was performed using silica gel (200−300 mesh) purchased from Qingdao Haiyang Chemical Co. Ltd. The purity of the samples was determined by high-performance liquid chromatography (HPLC), conducted on a Shimadzu LC-20AT series system with a TC-C18 column (4.6 mm × 250 mm, 5 μm). The samples were eluted with a 60:40 acetonitrile/H_2O mixture at a flow rate of 0.5 mL/min, and was detected at a wavelength of 254 nm. The purity of all biologically evaluated compounds is greater than 95%. The ^{1}H NMR and ^{13}C NMR spectra were recorded using TMS as the internal standard on a Bruker BioSpin GmbH spectrometer at 400 and 100 MHz, respectively, and the coupling constants are reported in hertz. The high-resolution mass spectra were obtained using a Shimadzu LCMS-IT-TOF mass spectrometer.

*4-bromo-2-methoxyphenol (**2**).* To a solution of guaiacol (124 mg, 1 mmol) in CH_3CN (20 mL) at 0 °C, bromosuccinimide (180 mg, 1 mmol) was added. After

stirring for 30 min, the mixture was quenched with saturated sodium thiosulfate and then extracted with EtOAc for three times. The combined organic phase was washed with brine, dried over anhydrous sodium sulfate and concentrated. The crude product was purified by column chromatography (PE/EtOAc, 10:1) to provide **2**. White oil, 95% yield. ^{1}H NMR (400 MHz, $CDCl_3$) δ 7.06 – 6.91 (m, 2H), 6.80 (d, J = 8.3 Hz, 1H), 5.55 (s, 1H), 3.88 (s, 3H).

*4-bromo-2-methoxy-6-nitrophenol (**3**).*[17] To a stirred solution of **2** (203 mg, 1 mmol) in acetic acid (5 mL), 65% HNO_3 (0.097 mL, 1.2 mmol) was added in dropwise. After stirring at room temperature for 10 min, the mixture was poured into ice water. The resulting precipitate was filtered off, washed with water, and dried under vacuum to give the product, yellow solid, 96% yield. ^{1}H NMR (400 MHz, $CDCl_3$) δ 10.70 (s, 1H), 7.86 (d, J = 2.2 Hz, 1H), 7.21 (d, J = 2.2 Hz, 1H), 3.95 (s, 3H).

*5-bromo-1,2-dimethoxy-3-nitrobenzene (**4**).* A mixture of **3** (248 mg, 1 mmol), tetrabutylammonium iodide (369 mg, 1 mmol), and KOH (112 mg, 2 mmol) in 10 mL of DMF was added iodomethane (141 mg, 1 mmol). The reaction mixture was stirred at 40 °C and monitored by TLC. After the completion of the reaction (48 h), ice water was added. The resulting precipitate was filtered off, washed with water, and dried under vacuum to give the product, yellow solid, 78% yield. ^{1}H NMR (400 MHz, $CDCl_3$) δ 7.76 (d, J = 2.2 Hz, 1H), 7.49 (d, J = 2.2 Hz, 1H), 3.89 (d, J = 8.8 Hz, 6H).

*5-bromo-2,3-dimethoxyaniline (**5**).*[18] Iron powder (280 mg, 5 mmol) was added to a mixture of **4** (260 mg, 1 mmol) in EtOH (15 mL) and AcOH (8 mL). The reaction was

stirred at rt for 3h, then neutralized with a saturated solution of $NaHCO_3$. After extraction with EtOAc, the organic layer was washed with brine, dried over anhydrous sodium sulfate, concentrated, and purified by column chromatography (PE/EtOAc, 5:1) to obtain **5**. Yellow oil, 68% yield. ^{1}H NMR (400 MHz, $CDCl_3$) δ 6.53 (d, J = 2.1 Hz, 1H), 6.45 (d, J = 2.1 Hz, 1H), 3.88 (s, 2H), 3.82 (d, J = 1.7 Hz, 3H), 3.79 (d, J = 1.8 Hz, 3H).

*5-bromo-1,2-dimethoxy-3-selenocyanatobenzene (**6**).* To a stirred solution of **5** (232 mg, 1mmol) in 10% HCl (2.5 mL) at 0 °C, sodium nitrite (83 mg, 1.2 mmol) was added and the reaction mixture was kept below 5 °C. After completion of the reaction, saturated sodium acetate was added to adjust pH at 6.0. Then, the solution of potassium selenocyanate (220 mg, 1.5 mmol) in water (1 mL) was added in dropwise. The reaction mixture was stirred at rt for 1 h, and the resulting precipitate was filtered off, washed with water, and dried under vacuum to give the product, orange solid, 78% yield. ^{1}H NMR (400 MHz, $CDCl_3$) δ 7.33 (d, J = 2.0 Hz, 1H), 7.02 (d, J = 2.1 Hz, 1H), 3.90 (s, 3H), 3.87 (s, 3H).

*1-(5-bromo-2,3-dimethoxyphenyl)-2-(4-bromo-2,6-dimethoxyphenyl)diselane (**7**).* KOH (112 mg, 2 mmol) was added to a solution of **6** (321 mg, 1 mmol) in MeOH (5mL). The mixture was stirred for 1h, and the resulting orange-yellow precipitate was filtered off, washed with MeOH, and dried under vacuum to give the product, orange-yellow solid, 72% yield. ^{1}H NMR (400 MHz, $CDCl_3$) δ 7.23 (d, J = 2.2 Hz, 1H), 6.92 (d, J = 2.1 Hz, 1H), 3.92 (s, 3H), 3.85 (s, 3H).

*(5-bromo-2,3-dimethoxyphenyl)(methyl)selane (**8**)*.[19] To a solution of diselenide **6** (590 mg, 1 mmol) in ethanol/water (1:1, 8 mL), $NaBH_4$ (76 mg, 2 mmol) was added in portions, and the mixture was stirred for 20 min. Iodomethane (141 mg, 1 mmol) was added and the reaction was stirred at rt for 1 h. After completion of the reaction, water was added, and the mixture was extracted with ethyl acetate for three times. The organic phase was washed with brine and dried over anhydrous sodium sulfate. The evaporation of the solvents gave the crude products which were purified by silica gel column (PE/EtOAc, 10:1) to afford **8**, colorless oil, 89% yield. ^{1}H NMR (400 MHz, $CDCl_3$) δ 6.88 (q, J = 2.2 Hz, 2H), 3.84 (s, 3H), 3.83 (s, 3H), 2.26 (s, 3H).

General Procedures for the Preparation of 9a-i.[20] Under an argon atmosphere, **8** (403 mg, 1.3 mmol) was dissolved in dry THF (20 mL) and then the solution was cooled to -78 °C. N-BuLi (1.3 mmol) was slowly added to the mixture and stirred for 0.5 h. Then, substituted benzaldehyde (1 mmol) in THF solution was added in dropwise. After stirred for 12 h, the reaction was quenched by the addition of saturated ammonium chloride solution, and extracted with ethyl acetate. The organic phase was dried over anhydrous sodium sulfate, and the solvent was removed under vacuum. The residue was purified by flash column chromatography (PE/EtOAc, 3:1) to give the according products.

*5-((3,4-dimethoxy-5-(methylselanyl)phenyl)(hydroxy)methyl)-2-methoxyphenol (**9a**)*. Colorless oil, yield: 69%. ^{1}H NMR (400 MHz, $CDCl_3$) δ 6.92 (ddd, J = 20.1, 2.0, 1.1 Hz, 2H), 6.84 (ddd, J = 7.3, 2.0, 1.0 Hz, 1H), 6.79 (dd, J = 2.1, 1.0 Hz, 1H), 6.67 (d, J

= 7.5 Hz, 1H), 5.98 – 5.94 (m, 1H), 5.92 (s, 1H), 3.90 (s, 3H), 3.85 (s, 6H), 2.22(s, 3H).

(3,4-dimethoxy-5-(methylselanyl)phenyl)(3-fluoro-4-methoxyphenyl)methanol ***(9b)***. Colorless oil, yield: 69%. ^{1}H NMR (400 MHz, $CDCl_3$) δ 7.05 (ddd, J = 7.5, 1.9, 0.9 Hz, 1H), 6.94 (dd, J = 2.0, 1.1 Hz, 1H), 6.92 – 6.86 (m, 2H), 6.86 – 6.80 (m, 1H), 5.98 – 5.92 (m, 1H), 4.50 (d, J = 4.9 Hz, 1H), 3.90 (s, 3H), 3.84 (d, J = 4.9 Hz, 6H), 2.23 (s, 3H).

(3-chloro-4-methoxyphenyl)(3,4-dimethoxy-5-(methylselanyl)phenyl)methanol ***(9c)***. Colorless oil, yield: 68%. ^{1}H NMR (400 MHz, $CDCl_3$) δ 7.40 (d, J = 2.1 Hz, 1H), 7.21 (dd, J = 8.6, 2.2 Hz, 1H), 6.89 (d, J = 8.3 Hz, 1H), 6.77 (dd, J = 18.3, 1.7 Hz, 2H), 5.71 (d, J = 3.4 Hz, 1H), 3.89 (s, 3H), 3.85 (s, 3H), 3.83 (s, 3H), 2.24 (s, 3H).

(3-bromo-4-methoxyphenyl)(3,4-dimethoxy-5-(methylselanyl)phenyl)methanol ***(9d)*** Colorless oil, yield: 69%. ^{1}H NMR (400 MHz, $CDCl_3$) δ 7.37 (dd, J = 2.0, 1.0 Hz, 1H), 7.22 (ddd, J = 7.5, 2.0, 1.0 Hz, 1H), 6.98 – 6.88 (m, 3H), 5.98 – 5.92 (m, 1H), 3.90 (d, J = 4.9 Hz, 6H), 3.85 (s, 3H), 2.22 (s, 3H).

(3,4-dimethoxy-5-(methylselanyl)phenyl)(4-methoxyphenyl)methanol ***(9e)***. Colorless oil, yield: 69%. ^{1}H NMR (400 MHz, $CDCl_3$) δ 7.31 – 7.26 (m, 2H), 6.92 – 6.84 (m, 2H), 6.83 – 6.73 (m, 2H), 5.74 (d, J = 3.4 Hz, 1H), 2.22 (s, 3H).

(3,4-dimethoxy-5-(methylselanyl)phenyl)(2,3,4-trimethoxyphenyl)methanol ***(9f)***. Colorless oil, yield: 68%. ^{1}H NMR (400 MHz, $CDCl_3$) δ 6.91 (d, J = 8.6 Hz, 1H), 6.81 (d, J = 5.2 Hz, 2H), 6.64 (d, J = 8.5 Hz, 1H), 5.89 (d, J = 5.7 Hz, 1H), 3.85 (d, J = 5.2 Hz, 9H), 3.82 (s, 3H), 3.76 (s, 3H), 2.21 (s, 3H).

(3,4-dimethoxy-5-(methylselanyl)phenyl)(3,4-dimethoxyphenyl)methanol ***(9g)***. Colorless oil, yield: 68%. ^{1}H NMR (400 MHz, $CDCl_3$) δ 6.99 – 6.92 (m, 3H), 6.90 (dd, J = 2.1, 1.1 Hz, 1H), 6.84 (d, J = 7.6 Hz, 1H), 5.98 – 5.92 (m, 1H), 3.92 – 3.83 (m, 12H), 2.22 (s, 3H).

(3,4-dimethoxy-5-(methylselanyl)phenyl)(3,4,5-trimethoxyphenyl)methanol ***(9h)***. Colorless oil, yield: 71%. ^{1}H NMR (400 MHz, $CDCl_3$) δ 6.92 (ddd, J = 20.2, 2.0, 1.1 Hz, 2H), 6.62 (d, J = 0.9 Hz, 2H), 5.98 – 5.92 (m, 1H), 3.90 (s, 3H), 3.84 (d, J = 4.9 Hz, 12H), 2.24 (s, 3H).

(3,4-dimethoxy-5-(methylselanyl)phenyl)(4-methoxy-3-methylphenyl)methanol ***(9i)***. Colorless oil, yield: 70%. ^{1}H NMR (400 MHz, $CDCl_3$) δ 7.14 (d, J = 7.3 Hz, 2H), 6.82 (d, J = 1.7 Hz, 1H), 6.78 (d, J = 7.0 Hz, 2H), 5.71 (d, J = 3.1 Hz, 1H), 3.84 (s, 3H), 3.82 (d, J = 1.8 Hz, 6H), 2.23 (s, 3H), 2.20 (s, 3H).

General procedures for the preparation of 10a-i.[21] 2-iodoxybenzoic acid (560 mg, 2 mmol) was added in portions to a solution of **9** (1 mmol) in THF (10 mL). The reaction mixture was allowed to stirred for 3h, and the resulting precipitate was filtered off. The filtrate was concentrated and purified by flash column chromatography (PE/EtOAc, 3:1) to give the target compound.

(3,4-dimethoxy-5-(methylselanyl)phenyl)(3-hydroxy-4-methoxyphenyl)methanone ***(10a)***. White solid, yield: 78%.^{1}H NMR (400 MHz, $CDCl_3$) δ 7.45 (d, J = 2.1 Hz, 1H), 7.39 (dd, J = 8.3, 2.1 Hz, 1H), 7.21 (q, J = 1.9 Hz, 2H), 6.92 (d, J = 8.4 Hz, 1H), 5.76 (d, J = 1.0 Hz, 1H), 3.99 (s, 3H), 3.95 (s, 3H), 3.89 (s, 3H), 2.24 (s, 3H).^{13}C NMR (100 MHz, $CDCl_3$) δ 194.5, 151.8, 150.3, 149.5, 145.3, 134.5, 131.0, 127.6, 123.8,

122.1, 116.2, 111.5, 109.7, 60.2, 56.13, 56.05, 5.1. HRMS (ESI) (*m/z*) $[M+H]^+$ calcd for $C_{17}H_{18}O_5Se$, 383.0393; found, 383.0408. Purity: 96.1% (by HPLC).

(3,4-dimethoxy-5-(methylselanyl)phenyl)(3-fluoro-4-methoxyphenyl)methanone ***(10b)***. White solid, yield: 76%. ^{1}H NMR (400 MHz, $CDCl_3$) δ 7.65 – 7.57 (m, 2H), 7.23 – 7.17 (m, 2H), 7.03 (t, J = 8.4 Hz, 1H), 3.98 (s, 3H), 3.96 (s, 3H), 3.90 (s, 3H), 2.24 (s, 3H). ^{13}C NMR (100 MHz, $CDCl_3$) δ 193.3, 152.5, 151.0, 150.6, 149.7, 134.0, 130.4, 127.8, 127.5, 122.1, 117.8, 112.2, 111.5, 60.2, 56.3, 56.1, 5.1. HRMS (ESI) (*m/z*) $[M+H]^+$ calcd for $C_{17}H_{17}O_4FSe$, 385.0350; found, 385.0368. Purity: 96.3% (by HPLC).

(3-chloro-4-methoxyphenyl)(3,4-dimethoxy-5-(methylselanyl)phenyl)methanone ***(10c)***. White solid, yield: 79%.^{1}H NMR (400 MHz, $CDCl_3$) δ 7.90 (d, J = 2.2 Hz, 1H), 7.74 (dd, J = 8.6, 2.1 Hz, 1H), 7.23 – 7.16 (m, 2H), 7.00 (d, J = 8.6 Hz, 1H), 4.00 (s, 3H), 3.96 (s, 3H), 3.90 (s, 3H), 2.24 (s, 3H).^{13}C NMR (100 MHz, $CDCl_3$) δ 193.1, 158.4, 152.0, 149.9, 133.9, 132.3, 130.9, 130.5, 127.8, 122.7, 122.2, 111.6, 111.1, 60.2, 56.4, 56.1, 5.1. HRMS (ESI) (*m/z*) $[M+H]^+$ calcd for $C_{17}H_{17}O_4ClSe$, 401.0052; found, 401.0068. Purity: 97.3% (by HPLC).

(3-bromo-4-methoxyphenyl)(3,4-dimethoxy-5-(methylselanyl)phenyl)methanone ***(10d)***.White solid, yield: 81%.^{1}H NMR (400 MHz, $CDCl_3$) δ 8.07 (d, J = 2.1 Hz, 1H), 7.78 (dd, J = 8.5, 2.1 Hz, 1H), 7.24 – 7.15 (m, 2H), 6.97 (d, J = 8.6 Hz, 1H), 3.99 (s, 3H), 3.96 (s, 3H), 3.90 (s, 3H), 2.24 (s, 3H).^{13}C NMR (100 MHz, $CDCl_3$) δ 193.0, 159.3, 152.0, 149.9, 135.4, 133.9, 131.34, 131.25, 127.9, 122.3, 111.7, 111.6, 111.0,

60.2, 56.5, 56.1, 5.1. HRMS (ESI) (*m/z*) $[M+H]^+$ calcd for $C_{17}H_{17}O_4SeBr$, 444.9546; found, 444. 9564. Purity: 96.5% (by HPLC).

*(3,4-dimethoxy-5-(methylselanyl)phenyl)(4-methoxyphenyl)methanone (**10e**).* White solid, yield: 78%. ^{1}H NMR (400 MHz, CDCl3) δ 7.82 (d, J = 8.4 Hz, 2H), 7.24 – 7.16 (m, 2H), 6.97 (d, J = 8.5 Hz, 2H), 3.95 (s, 3H), 3.89 (d, J = 1.4 Hz, 6H), 2.23 (s, 3H).^{13}C NMR (100 MHz, $CDCl_3$) δ 194.3, 163.2, 151.8, 149.4, 134.6, 132.4, 130.2, 127.6, 122.1, 113.6, 111.5, 60.1, 56.0, 55.5, 5.0. HRMS (ESI) (*m/z*) $[M+H]^+$ calcd for $C_{17}H_{18}O_4Se$, 367.0444; found, 367. 0455. Purity: 95.4% (by HPLC).

*(3,4-dimethoxy-5-(methylselanyl)phenyl)(2,3,4-trimethoxyphenyl)methanone (**10f**).* White solid, yield: 80%. ^{1}H NMR (400 MHz, $CDCl_3$) δ 7.30 (d, J = 1.7 Hz, 1H), 7.23 (d, J = 1.7 Hz, 1H), 7.11 (d, J = 8.6 Hz, 1H), 6.73 (d, J = 8.6 Hz, 1H), 3.94 (d, J = 3.0 Hz, 6H), 3.90 (s, 3H), 3.88 (s, 3H), 3.79 (s, 3H), 2.20 (s, 3H).^{13}C NMR (100 MHz, $CDCl_3$) δ 194.1, 156.1, 152.6, 151.8, 150.3, 142.1, 134.6, 127.4, 126.3, 124.9, 122.8, 111.2, 106.7, 61.9, 61.0, 60.2, 56.1, 56.0, 5.0. HRMS (ESI) (*m/z*) $[M+H]^+$ calcd for $C_{19}H_{22}O_6Se$, 427.0655; found, 427.0670. Purity: 98.3% (by HPLC).

*(3,4-dimethoxy-5-(methylselanyl)phenyl)(3,4-dimethoxyphenyl)methanone (**10g**).* White solid, yield: 78%. ^{1}H NMR (400 MHz, $CDCl_3$) δ 7.47 (s, 1H), 7.44 – 7.36 (m, 1H), 7.22 (s, 2H), 6.91 (d, J = 8.3 Hz, 1H), 3.97 (s, 3H), 3.95 (s, 6H), 3.90 (s, 3H), 2.25 (s, 3H).^{13}C NMR (100 MHz, $CDCl_3$) δ 194.3, 153.0, 151.8, 149.4, 148.9, 134.6, 130.2, 127.6, 125.2, 122.0, 112.2, 111.5, 109.8, 60.1, 56.5, 56.1, 56.0, 5.0. HRMS (ESI) (*m/z*) $[M+H]^+$ calcd for $C_{18}H_{20}O_5Se$, 397.0550; found, 397.0571. Purity: 95.6% (by HPLC).

(3,4-dimethoxy-5-(methylselanyl)phenyl)(3,4,5-trimethoxyphenyl)methanone ***(10h)***. White solid, yield: 82%. ^{1}H NMR (400 MHz, $CDCl_3$) δ 7.27 (d, J = 1.6 Hz, 1H), 7.25 (d, J = 1.9 Hz, 1H), 7.07 (s, 2H), 3.96 (s, 3H), 3.95 (s, 3H), 3.90 (s, 3H), 3.89 (s, 6H), 2.25 (s, 3H). ^{13}C NMR (100 MHz, $CDCl_3$) δ 194.3, 152.9, 151.9, 149.9, 142.1, 134.0, 132.7, 127.8, 122.5, 111.8, 107.8, 61.0, 60.2, 56.4, 56.1, 5.1. HRMS (ESI) (*m/z*) $[M+H]^+$ calcd for $C_{19}H_{22}O_6Se$, 427.0655; found, 427.0676. Purity: 95.6% (by HPLC).

(3,4-dimethoxy-5-(methylselanyl)phenyl)(4-methoxy-3-methylphenyl)methanone ***(10i)***. White solid, yield: 79%. ^{1}H NMR (400 MHz, $CDCl_3$) δ 7.68 (d, J = 10.1 Hz, 2H), 7.21 (d, J = 2.3 Hz, 2H), 6.87 (d, J = 8.3 Hz, 1H), 3.95 (s, 3H), 3.92 (s, 3H), 3.89 (s, 3H), 2.27 (s, 3H), 2.24 (s, 3H). ^{13}C NMR (100 MHz, $CDCl_3$) δ 194.6, 161.5, 151.8, 149.4, 134.8, 132.7, 130.4, 129.7, 127.5, 126.8, 122.2, 111.6, 109.0, 60.2, 56.1, 56.0, 55.6, 16.2, 5.0. HRMS (ESI) (*m/z*) $[M+H]^+$ calcd for $C_{18}H_{20}O_4Se$, 381.0600; found, 381.0614. Purity: 99.0% (by HPLC).

General Procedures for the Preparation of 11a-i.[9] Under an argon atmosphere, methyltriphenylphosphonium bromide (176 mg, 2 mmol) was dissolved in dry THF (30 mL) and then the mixture was cooled to -78 °C. N-BuLi (2 mmol) was slowly added to the mixture, then warmed to rt and stirred for 0.5 h. Afterward, the mixture was cooled to -78 °C again, and a solution of **10** (1 mmol) in THF (5 mL) was added in dropwise. After stirred for another 0.5 h, the resulting solution was warmed to room temperature and stirred for 12 h. The reaction mixture was quenched by the addition of saturated ammonium chloride solution, and extracted by ethyl acetate. The organic layers were dried over anhydrous sodium sulfate, and the solvent was

removed under vacuum. The residue was purified by flash column chromatography (petroleum/ethyl acetate, 3:1) to give the target product.

5-(1-(3,4-dimethoxy-5-(methylselanyl)phenyl)vinyl)-2-methoxyphenol ***(11a)***. White solid, yield: 72%. ^{1}H NMR (400 MHz, $CDCl_3$) δ 6.97 (d, *J* = 1.9 Hz, 1H), 6.84 – 6.78 (m, 3H), 6.70 (d, *J* = 1.8 Hz, 1H), 5.59 (s, 1H), 5.39 (d, *J* = 1.2 Hz, 1H), 5.30 (d, *J* = 1.2 Hz, 1H), 3.92 (s, 3H), 3.89 (s, 3H), 3.80 (s, 3H), 2.21 (s, 3H). ^{13}C NMR (100 MHz, $CDCl_3$) *δ* 151.8, 149.1, 146.4, 146.1, 145.2, 138.6, 134.6, 127.0, 120.2, 112.0, 114.4, 113.0, 110.6, 110.1, 60.1, 56.0, 55.9, 5.0. HRMS (ESI) (*m/z*) $[M+H]^+$ calcd for $C_{18}H_{20}O_4Se$, 381.0600; found, 381.0621. Purity: 98.6% (by HPLC).

(5-(1-(3-fluoro-4-methoxyphenyl)vinyl)-2,3-dimethoxyphenyl)(methyl)selane ***(11b)***. White solid, yield: 73%.^{1}H NMR (400 MHz, $CDCl_3$) *δ* 7.17 – 7.02 (m, 2H), 6.91 (t, *J* = 8.6 Hz, 1H), 6.76 (d, *J* = 1.9 Hz, 1H), 6.68 (d, *J* = 1.9 Hz, 1H), 5.39 (d, *J* = 1.0 Hz, 1H), 5.34 (d, *J* = 1.0 Hz, 1H), 3.90 (d, *J* = 8.0 Hz, 6H), 3.81 (s, 3H), 2.21 (s, 3H).^{13}C NMR (100 MHz, $CDCl_3$) *δ* 152.0, 151.9, 148.2, 147.4, 146.3, 138.1, 134.3, 127.3, 124.0, 119.9, 115.8, 113.6, 112.8, 110.5, 60.1, 56.3, 55.9, 5.0. HRMS (ESI) (*m/z*) $[M+H]^+$ calcd for $C_{18}H_{19}O_3FSe$, 383.0557; found, 383.0579. Purity: 98.4% (by HPLC).

(5-(1-(3-chloro-4-methoxyphenyl)vinyl)-2,3-dimethoxyphenyl)(methyl)selane ***(11c)***. White solid, yield: 73%. ^{1}H NMR (400 MHz, $CDCl_3$) *δ* 7.40 (d, *J* = 2.2 Hz, 1H), 7.20 (dd, *J* = 8.5, 2.2 Hz, 1H), 6.88 (d, *J* = 8.6 Hz, 1H), 6.76 (d, *J* = 1.9 Hz, 1H), 6.68 (d, *J* = 1.9 Hz, 1H), 5.38 (d, *J* = 1.1 Hz, 1H), 5.34 (d, *J* = 1.1 Hz, 1H), 3.92 (s, 3H), 3.90 (s, 3H), 3.81 (s, 3H), 2.21 (s, 3H). ^{13}C NMR (100 MHz, $CDCl_3$) *δ* 154.7, 151.9,

148.1, 146.2, 138.1, 134.6, 129.9, 127.6, 127.3, 122.2, 119.8, 113.6, 111.6, 110.4, 60.1, 56.2, 55.9, 5.0. HRMS (ESI) (*m/z*) $[M+H]^+$ calcd for $C_{18}H_{19}O_3ClSe$, 399.0259; found, 399.0285. Purity: 95.5% (by HPLC).

(5-(1-(3-bromo-4-methoxyphenyl)vinyl)-2,3-dimethoxyphenyl)(methyl)selane ***(11d)***. White solid, yield: 77%. ^{1}H NMR (400 MHz, $CDCl_3$) δ 7.50 (d, J = 2.2 Hz, 1H), 7.16 (dd, J = 8.6, 2.2 Hz, 1H), 6.78 (d, J = 8.6 Hz, 1H), 6.68 (d, J = 1.8 Hz, 1H), 6.60 (d, J = 1.9 Hz, 1H), 5.30 (d, J = 1.1 Hz, 1H), 5.26 (d, J = 1.1 Hz, 1H), 3.83 (d, J = 8.2 Hz, 6H), 3.73 (s, 3H), 2.13 (s, 3H). ^{13}C NMR (100 MHz, $CDCl_3$) δ 155.6, 151.9, 147.9, 146.2, 138.1, 135.1, 132.9, 128.4, 127.4, 119.8, 113.7, 111.42, 111.37, 110.4, 60.1, 56.3, 55.9, 5.0. HRMS (ESI) (*m/z*) $[M+H]^+$ calcd for $C_{18}H_{19}O_3SeBr$, 442.9753; found, 442.9750. Purity: 95.4% (by HPLC).

(2,3-dimethoxy-5-(1-(4-methoxyphenyl)vinyl)phenyl)(methyl)selane ***(11e)***. White solid, yield: 73%. ^{1}H NMR (400 MHz, $CDCl_3$) δ 7.36 – 7.27 (m, 2H), 6.92 – 6.82 (m, 2H), 6.79 (d, J = 1.9 Hz, 1H), 6.71 (d, J = 1.9 Hz, 1H), 5.38 (d, J = 1.2 Hz, 1H), 5.31 (d, J = 1.3 Hz, 1H), 3.89 (s, 3H), 3.83 (s, 3H), 3.80 (s, 3H), 2.21 (s, 3H).^{13}C NMR (100 MHz, $CDCl_3$) δ 159.4, 151.8, 149.1, 146.1, 138.7, 133.6, 129.3, 127.1, 119.9, 113.5, 112.6, 110.5, 60.1, 55.9, 55.3, 5.0. HRMS (ESI) (*m/z*) $[M+H]^+$ calcd for $C_{18}H_{20}O_3Se$, 365.0651; found, 365.0647. Purity: 97.4% (by HPLC).

(2,3-dimethoxy-5-(1-(2,3,4-trimethoxyphenyl)vinyl)phenyl)(methyl)selane ***(11f)***. White solid, yield: 78%. ^{1}H NMR (400 MHz, $CDCl_3$) δ 6.83 (d, J = 1.9 Hz, 1H), 6.72 (d, J = 1.9 Hz, 1H), 6.57 (s, 2H), 5.45 – 5.36 (m, 2H), 3.89 (d, J = 5.8 Hz, 6H), 3.82 (d, J = 6.2 Hz, 9H), 2.23 (s, 3H).^{13}C NMR (100 MHz, $CDCl_3$) δ 152.9, 151.9, 149.6,

146.4, 138.1, 138.1, 136.8, 127.2, 120.1, 113.7, 110.6, 105.8, 60.9, 60.1, 56.3, 56.0, 5.0. HRMS (ESI) (*m/z*) $[M+H]^+$ calcd for $C_{20}H_{24}O_5Se$, 425.0863; found, 425.0901. Purity: 98.2% (by HPLC).

(5-(1-(3,4-dimethoxyphenyl)vinyl)-2,3-dimethoxyphenyl)(methyl)selane ***(11g)***. White solid, yield: 75%. ^{1}H NMR (400 MHz, $CDCl_3$) δ 6.95 – 6.87 (m, 2H), 6.86 – 6.77 (m, 2H), 6.72 (d, J = 1.9 Hz, 1H), 5.39 (d, J = 1.3 Hz, 1H), 5.34 (d, J = 1.2 Hz, 1H), 3.90 (d, J = 5.0 Hz, 6H), 3.85 (s, 3H), 3.80 (s, 3H), 2.21 (s, 3H).^{13}C NMR (100 MHz, $CDCl_3$) δ 151.8, 149.3, 148.9, 148.5, 146.1, 138.5, 134.0, 127.1, 121.0, 119.9, 112.9, 111.3, 110.7, 110.5, 60.1, 56.0, 55.9, 5.0. HRMS (ESI) (*m/z*) $[M+H]^+$ calcd for $C_{19}H_{22}O_4Se$, 395.0757; found, 395.0782. Purity: 95.9% (by HPLC).

(2,3-dimethoxy-5-(1-(3,4,5-trimethoxyphenyl)vinyl)phenyl)(methyl)selane ***(11h)***. White solid, yield: 75%.^{1}H NMR (400 MHz, $CDCl_3$) δ 6.83 (d, J = 1.9 Hz, 1H), 6.72 (d, J = 1.9 Hz, 1H), 6.57 (s, 2H), 5.45 – 5.36 (m, 2H), 3.89 (d, J = 5.8 Hz, 6H), 3.82 (d, J = 6.2 Hz, 9H), 2.23 (s, 3H). ^{13}C NMR (100 MHz, $CDCl_3$) δ 152.9, 151.9, 149.6, 146.4, 138.10, 138.08, 136.8, 127.2, 120.1, 113.7, 110.6, 105.8, 60.9, 60.1, 56.3, 56.0, 5.0. HRMS (ESI) (*m/z*) $[M+H]^+$ calcd for $C_{20}H_{24}O_5Se$, 425.0863; found, 425.0867. Purity: 95.1% (by HPLC).

(2,3-dimethoxy-5-(1-(4-methoxy-3-methylphenyl)vinyl)phenyl)(methyl)selane ***(11i)***. White solid, yield: 75%. ^{1}H NMR (400 MHz, $CDCl_3$) δ 7.20 – 7.07 (m, 2H), 6.83 – 6.75 (m, 2H), 6.71 (d, J = 1.9 Hz, 1H), 5.37 (d, J = 1.4 Hz, 1H), 5.28 (d, J = 1.3 Hz, 1H), 3.89 (s, 3H), 3.85 (s, 3H), 3.80 (s, 3H), 2.21 (d, J = 1.1 Hz, 6H). ^{13}C NMR (100 MHz, $CDCl_3$) δ 157.6, 151.8, 149.3, 146.1, 138.9, 133.1, 130.4, 127.0, 126.7, 126.2,

120.0, 112.5, 110.6, 109.4, 60.1, 55.9, 55.4, 16.3, 5.0. HRMS (ESI) (*m/z*) $[M+H]^+$ calcd for $C_{19}H_{22}O_3Se$, 379.0808; found, 379.0814. Purity: 96.0% (by HPLC).

*5-(1-(3,4-dimethoxy-5-(methylselanyl)phenyl)vinyl)-2-methoxyphenyl diethyl phosphate (**11aa**)*. To a solution of **11a** (379 mg, 1 mmol) in CH_2Cl_2 (20 mL), triethylamine (0.8 mL, 6 mmol) was added in dropwise. The reaction mixture was cooled to 0 °C, and diethyl phosphite (0.5 mL, 4 mmol) in CCl_4 (1.9 mL, 10 mmol) was added. The reaction mixture was stirred at 0 °C for 24 h, then, quenched with water. The mixture was extracted with CH_2Cl_2 for three times, and the organic phase was washed with brine and dried over anhydrous sodium sulfate. After evaporation of the solvent, the product was purified by silica gel column (PE/EtOAc, 3:1) to give the target compound. Colorless oil, 92% yield. ^{1}H NMR (400 MHz, $CDCl_3$) δ 7.12 (ddd, J = 8.4, 2.2, 1.1 Hz, 1H), 6.90 (d, J = 8.5 Hz, 1H), 6.74 (dd, J = 30.1, 1.8 Hz, 2H), 5.36 (dd, J = 27.0, 1.1 Hz, 2H), 4.34 – 4.12 (m, 4H), 3.89 (d, J = 1.8 Hz, 6H), 3.81 (s, 3H), 1.34 (ddd, J = 8.1, 6.6, 1.1 Hz, 6H).

*Sodium 5-(1-(3,4-dimethoxy-5-(methylselanyl)phenyl)vinyl)-2-methoxyphenyl phosphate (**11ab**)*. Under nitrogen atmosphere, to the solution of **11aa** (515 mg, 1 mmol) in anhydrous CH_2Cl_2, TMSBr (1.9 mL, 20 mmol) was added. After stirring at rt for 12 h, the solvent was removed and then a solution of NaOH (80 mg, 2 mmol) was added in dropwise. After stirred for 30 min, the solvent was evaporated and the resulting pale yellow powder was recrystallized in CH_3CN/H_2O (3:1) to afford the target compound. Pale yellow solid, 89% yield. ^{1}H NMR (400 MHz, D_2O) δ 7.55 (s, 1H), 6.79 (d, J = 10.3 Hz, 2H), 6.76 – 6.62 (m, 2H), 5.37 (d, J = 81.2 Hz, 2H), 3.77 (s,

3H), 3.70 (d, J = 4.0 Hz, 6H), 2.08 (s, 3H). ^{13}C NMR (100 MHz, D_2O) δ 151.5, 149.9, 148.3, 145.1, 143.2, 139.6, 133.8, 126.7, 122.4, 120.1, 119.8, 114.1, 120.0, 111.1, 60.3, 56.0, 55.9, 4.7. HRMS (ESI) (*m/z*) $[M+H]^+$ calcd for $C_{18}H_{21}O_7PSe$, 461.0264; found, 461.0269. Purity: 99.6% (by HPLC).

*1-bromo-4-selenocyanatobenzene (**13**)*. Following the same synthetic procedures as those for **6**, 4-bromoaniline (**12**) was converted to **13**. Orange solid, 77% yield. ^{1}H NMR (400 MHz, $CDCl_3$) δ 7.57 – 7.53 (m, 2H), 7.53 – 7.49 (m, 2H).

*1,2-bis(4-bromophenyl)diselane (**14**)*. Following the same snythetic procedures as those for **7**, **13** was converted to **14**. Orange-yellow solid, 71% yield. ^{1}H NMR (400 MHz, $CDCl_3$) δ 7.47 – 7.42 (m, 2H), 7.41 – 7.37 (m, 2H).

*(4-bromophenyl)(methyl)selane (**15**)*. Following the same synthetic procedures as those for **8**, **14** was converted to **15**. Colorless oil, 82% yield.^{1}H NMR (400 MHz, $CDCl_3$) δ 7.12 – 7.06 (m, 2H), 7.04 – 6.96 (m, 2H), 2.49 (s, 3H).

*(4-(methylselanyl)phenyl)(3,4,5-trimethoxyphenyl)methanol (**16**)*. Following the same synthetic procedures as those for **9**, **15** was converted to **16**. Colorless oil, 70% yield. ^{1}H NMR (400 MHz, $CDCl_3$) δ 7.89 (d, J = 8.4 Hz, 2H), 7.62 (d, J = 8.4 Hz, 2H), 7.24 (s, 2H), 5.82 (d, J = 1.0 Hz, 1H) 3.97 (s, 3H), 3.92 (s, 6H), 2.47 (s, 3H).

*(4-(methylselanyl)phenyl)(3,4,5-trimethoxyphenyl)methanone (**17**)*. Following the same synthetic procedures as those for **10**, **16** was converted to **17**. White solid, 77% yield. ^{1}H NMR (400 MHz, $CDCl_3$) δ 7.70 (d, J = 8.4 Hz, 2H), 7.47 (d, J = 8.4 Hz, 2H), 7.04 (s, 2H), 3.94 (s, 3H), 3.88 (s, 6H), 2.43 (s, 3H). ^{13}C NMR (100 MHz, $CDCl_3$) δ 195.1, 152.9, 142.0, 139.2, 135.0, 132.7, 130.5, 128.5, 107.6, 61.0, 56.3, 6.5. HRMS

(ESI) (*m/z*) $[M+H]^+$ calcd for $C_{17}H_{18}O_4Se$, 367.0444; found, 367.0431. Purity: 97.2% (by HPLC).

*Methyl(4-(1-(3,4,5-trimethoxyphenyl)vinyl)phenyl)selane (**18**)*. Following the same synthetic procedures as those for **11**, **17** was converted to **18**. White solid, 73% yield. ^{1}H NMR (400 MHz, $CDCl_3$) δ 7.38 (d, J = 8.4 Hz, 2H), 7.26 (d, J = 8.4 Hz, 2H), 6.54 (s, 2H), 5.42 (d, J = 1.2 Hz, 1H), 5.39 (d, J = 1.2 Hz, 1H), 3.87 (s, 3H), 3.81 (s, 6H), 2.37 (s, 3H). ^{13}C NMR (100 MHz, $CDCl_3$) δ 152.9, 149.5, 139.1, 138.0, 137.0, 131.7, 129.8, 128.8, 113.7, 105.8, 60.9, 56.2, 7.0. HRMS (ESI) (*m/z*) $[M+H]^+$ calcd for $C_{18}H_{20}O_3Se$, 365.0651; found, 365.0647. Purity: 97.5% (by HPLC).

Sodium 2-methoxy-5-(1-(3,4,5-trimethoxyphenyl)vinyl)phenyl phosphate (*Iso*CA-4P). *Iso*CA-4P was synthesized using the same way as described in the reference 33. 88% yield. ^{1}H NMR (400 MHz, D_2O) δ 7.56 (s, 1H), 6.83 (d, J = 8.5 Hz, 1H), 6.70 (dd, J = 8.4, 2.2 Hz, 1H), 6.65 (s, 2H), 5.48 (s, 1H), 5.32 (s, 1H), 3.82 (s, 3H), 3.73 (d, J = 2.9 Hz, 9H). ^{13}C NMR (100 MHz, D_2O) δ 152.2, 149.9, 148.8, 143.2, 138.4, 136.5, 133.8, 122.4, 119.9, 114.0, 112.1, 106.2, 61.0, 56.1. HRMS (ESI) (*m/z*) $[M–H]^–$ calcd for $C_{18}H_{21}O_8P$, 395.0901; found, 395.0898. Purity: 99.1% (by HPLC).

BIOLOGY

Cell Lines and Culture. The human cancer cell lines (A549, HELA, HEPG2, RKO, LOVO, A2780, HCT116, MGC803, MCF7, MDAMB231, A549/CDDP, HEPG2/DOX) used in this study were purchased from the Laboratory Animal Service Center at Sun Yat-sen University (Guangzhou, China). Cell lines A549, HELA,

HEPG2, RKO, LOVO, MGC803, MCF7, and MDAMB231 were cultivated in DMEM containing 10% (v/v) heat-inactivated fetal bovine serum (FBS), 100 units/mL penicillin, and 100 μg/mL streptomycin. Cell lines HCT116, A2780, HEPG2/DOX, and A549/CDDP were cultivated in RPMI 1640 medium containing 10% (v/v) heat-inactivated FBS, 100 units/mL penicillin, and 100 mg/mL streptomycin. The cells were incubated at 37 °C under a 5% CO_2 and 90% relative humidity (RH) atmosphere.

Antibodies and Reagents. A commercial kit (cytoskeleton, cat. #B011P) used for the tubulin polymerisation assay was purchased from Cytoskeleton (Danvers, MA, USA). The FITC-conjugated mouse anti-tubulin antibody was purchased from Cell Signaling Technology (Danvers, MA, USA). The goat anti-mouse IgG/Alexa-Fluor 488 antibody was obtained from Invitrogen (Camarillo, California, USA). A purified brain tubulin polymerisation kit was purchased from Cytoskeleton (Danvers, MA, Q9 USA). Annexin-V/FITC and the cell cycle analysis kit were purchased from Keygen Biotech, China. MTT was purchased from Sigma, USA. A lipophilic cationic dye, 5,50,6,60-tetrachloro-1,10,3,30-tetraethyl-benzimidazolcarbocyanine (JC-1), was obtained from Beyotime, China. The mouse anti-Bcl-xl monoclonal antibody, mouse anti-α-tubulin monoclonal antibody, rabbit anti-Bad, rabbit anti-Bcl-2, rabbit anti-Cyclin B1, rabbit anti-Cdc2, rabbit anti-Cdc25C, mouse anti-β-tubulin, and the horseradish peroxidase-conjugated goat anti-mouse IgG secondary antibody were all obtained from Cell Signaling Technology (Danvers, MA, USA). CA-4P was purchased from MAYA Reagent (Zhejiang, China).

MTT Assay. Cells grown in the logarithmic phase were seeded into 96-well plates (5×10^3 cells/well) for 24 h, and then exposed to different concentrations of the test compounds for 48 h. After attached cells were incubated with 5 mg/mL MTT (Sigma, USA) for another 4 h, the suspension was discarded, and subsequently the dark blue crystals (formazan) were solubilized in dimethyl sulfoxide (DMSO). The absorbance of the solution at 570 nm was measured using a multifunction microplate reader (Molecular Devices, Flex Station 3), and each experiment was performed at least in triplicate. IC_{50} values, which represent the drug concentrations required to cause 50% cancer cell growth inhibition, were used to express the cytotoxic effects of each compound and were calculated with GraphPad Prism Software version 5.02 (GraphPad Inc., La Jolla, CA, USA).

In vitro Tubulin Polymerization Assay. A tubulin polymerization assay was performed by measuring the increase in fluorescence intensity, which can be easily recorded due to the incorporation of a fluorescent reporter, DAPI (4′,6-diamidino-2-phenylindole), a fluorophore that is known to be a DNA intercalator. A commercial kit (cytoskeleton, cat. #BK011P) was used for the tubulin polymerization. The final buffer used for tubulin polymerization contained 80.0 mM piperazine-N, N′-bis(2-ethanesulfonic acid) sequisodium salt (pH 6.9), 2.0 mM $MgCl_2$, 0.5 mM EGTA, 1 mM GTP, and 10.2% glycerol. First, 5 μL of the tested compounds at the indicated concentrations was added, and the mixture was warmed to 37 °C for 1 min; then, the reaction was initiated by the addition of 55 μL of the tubulin solution. The fluorescence intensity enhancement was recorded every 60 sec

for 90 min in a multifunction microplate reader (Molecular Devices, Flex Station 3) (emission wavelength at 410 nm, excitation wavelength at 340 nm). The Vmax was used to determine the concentration that inhibited tubulin polymerization by 50% (IC_{50}) and was calculated using GraphPad Prism Software version 5.02 (GraphPad Inc., La Jolla, CA, USA).

Immunofluorescence Microscopy. In a 10 mm confocal culture dish, 3×10^4 cells were grown for 24 h and then incubated in the presence/absence of compound **11a** at the indicated concentrations for another 8 h. After being washed with phosphate-buffered solution (PBS) and fixed in 4% pre-warmed (37 °C) paraformaldehyde for 15 min, the cells were permeabilized with 0.5% Triton X-100 for 15 min and blocked for 30 min in 10% goat serum. Then, the cells were incubated with mouse anti-tubulin antibody (CST, USA) at 4 °C overnight, washed with PBS three times, and incubated with goat anti-mouse IgG/Alexa-Fluor 488 antibody (Invitrogen, USA) for 1 h. The samples were immediately visualized on a Zeiss LSM 570 laser scanning confocal microscope (Carl Zeiss, Germany) after the nuclei were stained with Hoechst 33342 (Sigma, USA) in the dark at room temperature for 30 min.

Cell Cycle Analysis. A549 cells were seeded in 6-well plates (3×10^5 cells/well), incubated in the presence/absence of compound **11a** at the indicated concentrations for 12 or 24 h, harvested by centrifugation, and then fixed in ice-cold 70% ethanol overnight. After the ethanol was removed the next day, the cells were re-suspended in ice-cold PBS, treated with RNAse A (Keygen Biotech, China) at 37 °C for 30 min,

and then incubated with the DNA staining solution propidium iodide (PI, Keygen Biotech, China) at 4 °C for 30 min. Approximately 10,000 events were detected by flow cytometry (Beckman Coulter, Epics XL) at 488 nm. The data regarding the number of cells in different phases of the cell cycle were analysed using EXPO32 ADC analysis software.

Apoptosis Analysis. A549 cells were seeded in 6-well plates (3×10^5 cells/well), incubated in the presence/absence of compound **11a** at the indicated concentrations for 24 or 48 h. After incubation, cells were harvested and incubated with 5 μL of Annexin-V/FITC (Keygen Biotech, China) in binding buffer (10 mM HEPES, 140 mM NaCl, and 2.5 mM $CaCl_2$ at pH 7.4) at room temperature for 15 min. PI solution was then added to the medium for another 10 min-incubation. Almost 10,000 events were collected for each sample and analysed by flow cytometry (Beckman Coulter, Epics XL). The percentage of apoptotic cells was calculated using EXPO32 ADC Analysis software.

Mitochondrial Membrane Potential Assay. A lipophilic cationic dye, 5,5′,6,6′-tetrachloro-1,1′,3,3′-tetraethyl-benzimidazolcarbocyanine (JC-1, Beyotime, China) was used to monitor the level of MMP in the cells. At normal state, the MMP is high and JC-1 appears as aggregates, which indicated by red fluorescence. When apoptosis occurs, the MMP reduced and JC-1 displayed as monomers, which indicated by green fluorescence. Two methods including flow cytometry and fluorescence microscopy were used to detect the MMP. For flow cytometry analysis, A549 cells were plated in 6-well plates (3×10^5 cells/well) and incubated for 24 h,

and treated with compound **11a** at the indicated concentrations for 24 h. Then, the cells were harvested by centrifugation and incubated with JC-1 solution for 30 min. After briefly washing, the proportion of green and red fluorescence intensity were immediately detected and analyzed by flow cytometry. For the fluorescence microscopy detection, A549 cells were plated in 6-well plates (3×10^5 cells/well) and incubated for 24 h, and treated with **11a** at the indicated concentrations for another 24 h. Then, the cells were stained with 2 μM JC-1 at 37 °C for 30 min, washed with PBS, and then the cell nuclei were stained with Hoechst 33342 (Sigma, USA) for 10 min in the dark. The cell images were immediate detected by a fluorescence microscopy (EVOS FL Auto).

Metabolic Stability Study. *Preparation of rat liver microsomes.* Male Sprague–Dawley rats (250–310 g) were purchased from the Laboratory Animal Service Center at Sun Yat-sen University (Guangzhou, China). The rats were fasted for 12 h before the experiments. All procedures were under the Regulations of Experimental Animal Administration issued by the Ministry of Science and Technology of the People's Republic of China. Rat liver microsomes were prepared by differential centrifugation as described.[34] In brief, after the mice were sacrificed by decapitated, the liver were excised and weighted. Then the liver homogenates were centrifuged at 16, 000 *g* for 20 min at 4 °C in a Beckman centrifuge (Beckman Coulter, Inc., Fullerton, CA, USA) to harvest the supernatant. After the supernatant was centrifuged at 100,000 *g* for 60 min twice at 4 °C in a L8-70 Beckman ultracentrifuge (Beckman Coulter), the resultant precipitation was resuspended in Tris–HCl buffer containing 20% glycerine

and stored at -80 °C until use. The protein concentration was determined by the method of Bradford.[35]

In vitro metabolic stability study. Compounds were subjected to in *vitro* incubations with rat liver microsomes in NADPH regenerating system, which consisting of 1.3 mM $NADPNa_2$, 3.3 mM glucose-6-phosphate, 0.4 U/mL glucose-6-phosphate dehydrogenase, and 3.3 mM $MgCl_2$ in 100 mM potassium phosphate buffer, pH 7.4. The final incubation volume was set at 500 μL. After an appropriate volume of microsomes was added to give a final of protein concentration of 1 mg/mL, the mixture were shaken incubated in 37 °C for indicated time and was terminated by the addition of 500 μL of ice-cold acetonitrile. The mixture was then vortexed for 30 sec and centrifuged at 4 °C for 10 min at 12,500 rpm to harvest the supernatants. Control group were carried out in the absence of regenerating system or microsomes. The supernatant was then directly analyzed by HPLC-UV and liquid chromatography-mass spectrometry (LC-MS/MS).

Western Bolt Analysis. A549 cells (5.0×10^5 cells/dish) were incubated with or without **11a** at various concentrations for 12 h, 24 h, or 48 h. After incubation, the cells were collected by centrifugation and washed twice with phosphate-buffered saline chilled to 0°C. Then, the cells were homogenised in RIPA lysis buffer containing 150 mM NaCl, 50 mM Tris (pH 7.4), 1% (w/v) sodium deoxycholate, 1% (v/v) Triton X-100, 0.1% (w/v) SDS and 1 mM EDTA (Beyotime, China). The lysates were incubated on ice for 30 min, intermittently vortexed every 5 min, and

centrifuged at 12,500 *g* for 15 min to harvest the supernatants. Next, the protein concentrations were determined by a BCA Protein Assay Kit (Thermo Fisher Scientific, Rockford, Illinois, USA). The protein extracts were reconstituted in loading buffer containing 62 mM Tris–HCl, 2% SDS, 10% glycerol, and 5% b-mercaptoethanol (Beyotime, China), and the mixture was boiled at 100°C for 3 min. An equal amount of the proteins (50 mg) were separated by 8–12% sodium dodecyl sulphate-polyacrylamide gel electrophoresis (SDS-PAGE) and were transferred to nitrocellulose membranes (Amersham Biosciences, Little Chalfont, Buckingham-shire, UK). Then, the membranes were blocked with 5% non-fat dried milk in TBS containing 1% Tween-20 for 90 min at room temperature, and then were incubated overnight with specific primary antibodies (CST, USA) at 4 °C. After three washes in TBST, the membranes were incubated with the appropriate HRP-conjugated secondary antibodies at room temperature for 2 h. The blots were developed with enhanced chemiluminescence (Pierce, Rockford, Illinois, USA) and were detected by an LAS4000 imager (GE Healthcare, Waukesha, Wisconsin, USA). The intensities of the blots were quantified by ImageQuantTL (GE Healthcare) software.

Evaluation of *in vivo* Anti-Tumour Activity.

Animals and Implantation of Cancer Cells. Male BALB/c nude mice (5 weeks old, 18–22 g) were purchased and housed at the Laboratory Animal Service Center of Sun Yat-Sen University (Guangzhou, China) in pathogen-free condition, maintained at

constant room temperature and fed a standard rodent chow and water. 1×10^7 cells / mL A549 cells grown in logarithmic phase were harvested and resuspended in FBS-free DMEM medium. Then, 0.1 mL of the cell suspension was subcutaneously injected into the right flank of each mouse. After implantation, the tumour mass was measured with an electronic caliper twice a week, and the tumour volume was calculated according to the following formula: tumor volume (mm^3) = 0.5 × length × $width^2$.

Drug treatments and evaluation of in vivo anti-tumour activity. When the tumour volume was reached about 100 mm^3, the xenograft tumour-bearing nude mice were randomly placed into four groups at 9 mice per group: vehicle group, CA-4P group, *iso*CA-4P group, and **11ab** group. The reference compounds CA-4P, *iso*CA-4P and the test compound **11ab** were completely dissolved in isotonic saline. The mice were injected intraperitoneally (ip) at a dose of 30 mg/kg body weight every other day, whereas control group were treated with an equivalent volume of vehicle. Tumour volume and body weights were recorded every other day after drug treatment. At the end of the observation period, the animals were euthanized by cervical dislocation and the tumour bulks were peeled off conformed to the Guide for the Care and Use of Laboratory Animals as published by the US National Institutes of Health (NIH Publication No. 85-23, revised 1996) and approved by the Institutional Ethics Review Board of Sun Yat-Sen University, and the case number is IACUC-DD-17-0505.

Statistical Analysis. Data are shown as the means ± standard error of the mean (SEM) from at least three independent experiments. Statistical analysis was carryout out

using one-way analysis of variance followed by a Bonferroni posthoc for multiple group comparison or Student's unpaired *t*-test for two-group comparison in appropriate condition. Unless otherwise indicated, the differences were considered to be statistically significant at $P < 0.05$. The analyses were performed using GraphPad Prism Software version 5.02 (GraphPad Inc., La Jolla, CA, USA).

ASSOCIATED CONTENT

Supporting Information

^{1}H and ^{13}C NMR spectra, HPLC chromatograms, high resolution mass spectra for target compounds **10a–10i**, **11a–11i**, **17**, **18**, **11ab**, and *iso*CA-4P. Molecular formula strings for **10a–10i**, **11a–11i**, **17**, **18**, and **11ab**.

AUTHOR INFORMATION

Corresponding authors

*(X.-S. Li) Phone and fax: +86-20-39943050. E-mail: lixsh@mail.sysu.edu.cn.

*(S. Yin) Phone and fax: +86-20-39943090. E-mail: yinsh2@mail.sysu.edu.cn.

Author Contributions

†Y.-Q. Pang and B.-J. An contributed equally.

Notes

The authors declare no competing financial interest.

ACKNOWLEDGMENTS

The authors thank the National Natural Science Foundation of China (No. 81573302), National High Technology Research and Development Program of China (863 Projects, No. 2015AA020928), the Guangdong Natural Science Funds for Distinguished Young Scholar (No. 2014A030306047), Guangdong High-level personnel of special support program-Young top-notch talent project (2015TQ01R244), and Guangzhou Pearl River New Star Fund Science and Technology Planning Project (201610010111) for providing financial support to this work.

ABBREVIATIONS USED

MMP, mitochondrial membrane potential; CA-4, combretastatin A-4; *iso*CA-4, *iso*combretastatin A-4; COX, cyclo-oxygen-ase; SARs, structure and activity relationships; MTT, 3-(4,5-dimethyl-2-thiazolyl)-2,5-diphenyl-2-H-tetrazolium bromide; PI, propidium iodide; RF, resistant factor; RH, relative humidity; EGTA, ethylene glycol bis(β-aminoethyl ether)-N,N,N′,N′-tetraacetic acid; GTP, guanosine triphosphate; HRMS, high-resolution mass spectra; TLC, thin-layer chromatography; HPLC, high performance liquid chromatography; SDS-PAGE, sodium dodecyl sulphate-polyacrylamide gel electrophoresis.

REFERENCES

1. Prota, A. E.; Bargsten, K.; Zurwerra, D.; Field, J. J.; Díaz, J. F.; Altmann, K.-H.;

Steinmetz, M. O. Molecular mechanism of action of microtubule-stabilizing anticancer agents. *Science* **2013**, *339*, 587–590.

2. Schiff, P. B.; Fant, J.; Horwitz, S. B. Promotion of microtubule assembly in vitro by taxol. *Nature* **1979**, *277*, 665–667.

3. Bhattacharyya, B.; Panda, D.; Gupta, S.; Banerjee, M. Anti-mitotic activity of colchicine and the structural basis for its interaction with tubulin. *Med. Res. Rev.* **2008**, *28*, 155–183.

4. Jordan, M. A. Mechanism of action of antitumor drugs that interact with microtubules and tubulin. *Curr. Med. Chem. Anticancer Agents* **2002**, *2*, 1–17.

5. Pettit, G. R.; Cragg, G. M.; Herald, D. L.; Schmidt, J. M.; Lohavanijaya, P. Isolation and structure of combretastatin. *Can. J. Chem.* **1982**, *60*, 1374–1376.

6. Zweifel, M.; Jayson, G. C.; Reed, N. S.; Osborne, R.; Hassan, B.; Ledermann, J.; Shreeves, G.; Poupard, L.; Lu, S. P.; Balkissoon, J.; Chaplin, D. J.; Rustin, G. J. Phase II trial of combretastatin A4 phosphate, carboplatin, and paclitaxel in patients with platinum-resistant ovarian cancer. *Ann. Oncol.* **2011**, *22*, 2036–2041.

7. Pettit, G. R.; Toki., B. E.; Herald, D. L.; Boyd, M. R.; Hamel, E.; Pettit, R. K.; Chapuis, J. C. Antineoplastic agents. asymmetric hydroxylation of trans-Combretastatin A-4. *J. Med. Chem.* **1999**, *42*, 1459–1465.

8. Kaur, R.; Kaur, G.; Gill, R. K.; Soni, R.; Bariwal, J. Recent developments in tubulin polymerization inhibitors: An overview. *Eur. J Med. Chem.* **2014**, *87*, 89–124.

9. (a) Messaoudi, S.; Treguier, B.; Hamze, A.; Provot, O.; Peyrat, J. F.; De Losada, J. R.; Liu, J. M.; Bignon, J.; Wdzieczak-Bakala, J.; Thoret, S.; Dubois, J.; Brion, J. D.;

Alami, M. Isocombretastatins a versus combretastatins a: the forgotten *iso*CA-4 isomer as a highly promising cytotoxic and antitubulin agent. *J. Med. Chem.* **2009**, *52*, 4538–4542. (b) Alvarez, R.; Alvarez, C.; Mollinedo, F.; Sierra, B. G.; Medarde, M.; Pelaez, R. *Iso*combretastatins A: 1,1-diarylethenes as potent inhibitors of tubulin polymerization and cytotoxic compounds. *Bioorg. Med. Chem.* **2009**, *17*, 6422–6431. (c) Hamze, A.; Giraud, A.; Messaoudi, S.; Provot, O.; Peyrat, J. F.; Bignon, J.; Liu, J. M.; Wdzieczak-Bakala, J.; Thoret, S.; Dubois, J.; Brion, J. D.; Alami, M. Synthesis, biological evaluation of 1,1-diarylethylenes as a novel class of antimitotic agents. *ChemMedChem* **2009**, *4*, 1912–1924.

10. Clement, I. P.;Lisk., D. J.; Ganther, H. E. Activities of structurally-related lipophilic selenium compounds as cancer chempreventive agents. *Anticancer Res.* **1998**, *18*, 4019–4025.

11. Li, Z.; Carrier, L.; Belame, A.; Thiyagarajah, A.; Salvo, V. A.; Burow, M. E.; Rowan, B. G. Combination of methylselenocysteine with tamoxifen inhibits MCF-7 breast cancer xenografts in nude mice through elevated apoptosis and reduced angiogenesis. *Breast Cancer Res. Treat.* **2009**, *118*, 33–43.

12. Ip, C.; Ganther, H. E. Activity of methylated forms of selenium in cancer prevention. *Cancer Res.* **1990**, *50*, 1206–1211.

13. Gowda, R.; Madhunapantula, S. V.; Desai, D.; Amin, S.; Robertson, G. P. Simultaneous targeting of COX-2 and AKT using selenocoxib-1-GSH to inhibit melanoma. *Mol. Cancer Ther.* **2012**, *12*, 3–15.

14. dos Santos, E. A.; Hamel, E.; Bai, R.; Burnett, J. C.; Tozatti, C. S. S.; Bogo, D.;

Perdomo, R. T.; Antunes, A. M. M.; Marques, M. M.; Matos, M. F. C.; de Lima, D. P. Synthesis and evaluation of diaryl sulfides and diaryl selenide compounds for antitubulin and cytotoxic activity. *Bioorg. Med. Chem. Lett.* **2013**, *23*, 4669–4673.

15. Guan, Q.; Yang, F.; Guo, D.; Xu, J.; Jiang, M.; Liu, C.; Bao, K.; Wu, Y.; Zhang, W. Synthesis and biological evaluation of novel 3,4-diaryl-1,2,5-selenadiazol analogues of combretastatin A-4. *Eur. J. Med. Chem.* **2014**, *87*, 1–9.

16. Wen, Z.; Xu, J.; Wang, Z.; Qi, H.; Xu, Q.; Bai, Z.; Zhang, Q.; Bao, K.; Wu, Y.; Zhang, W. 3-(3,4,5-Trimethoxyphenylselenyl)-1H-indoles and their selenoxides as combretastatin A-4 analogs: microwave-assisted synthesis and biological evaluation. *Eur. J. Med. Chem.* **2015**, *90*, 184–194.

17. Kiss, L. E.; Ferreira, H. S.; Torrao, L.; Bonifacio, M. J.; Palma, P. N.; Soares-da-Silva, P.; Learmonth, D. A. Discovery of a long-acting, peripherally selective inhibitor of catechol-O-methyltransferase. *J. Med. Chem.* **2010**, *53*, 3396–3411.

18. Turkman, N.; Shavrin, A.; Ivanov, R. A.; Rabinovich, B.; Volgin, A.; Gelovani, J. G.; Alauddin, M. M. Fluorinated cannabinoid CB2 receptor ligands: synthesis and in vitro binding characteristics of 2-oxoquinoline derivatives. *Bioorg. Med. Chem.* **2011**, *19*, 5698–5707.

19. Wang, Z.; Wang, Y.; Li, W.; Mao, F.; Sun, Y.; Huang, L.; Li, X. Design, synthesis, and evaluation of multitarget-directed selenium-containing clioquinol derivatives for the treatment of Alzheimer's disease. *ACS Chem. Neurosci.* **2014**, *5*, 952–962.

20. Peng, Y.; Luo, Z. B.; Zhang, J. J.; Luo, L.; Wang, Y. W. Collective synthesis of several 2,7'-cyclolignans and their correlation by chemical transformations. *Org. Biomol. Chem.* **2013**, *11*, 7574−7586.

21. Tang, G. Z.; Nikolovska-Coleska, Z; Qiu, S.; Yang, C.-Y.; Guo, J.; Wang, S. M.;. Acylpyrogallols as inhibitors of antiapoptotic Bcl-2 proteins. *J. Med. Chem.* **2008**, *51*, 717−720.

22. Xu, Q.; Wang, Y.; Xu, J.; Sun, M.; Tian, H.; Zuo, D.; Guan, Q.; Bao, K.; Wu, Y.; Zhang, W. Synthesis and bioevaluation of 3,6-diaryl-[1,2,4]triazolo[4,3-b] pyridazines as antitubulin agents. *ACS Med. Chem. Lett.* **2016**, *7*, 1202−1206.

23. Liu, Y. N.; Wang, J. J.; Ji, Y. T.; Zhao, G. D.; Tang, L. Q.; Zhang, C. M.; Guo, X. L.; Liu, Z. P. Design, synthesis, and biological evaluation of 1-methyl-1,4-dihydroindeno[1,2-c]pyrazole analogues as potential anticancer agents targeting tubulin colchicine binding site. *J. Med. Chem.* **2016**, *59*, 5341−5355.

24. Bonne, D.; Heuséle, C.; Simon, C.; Pantaloni, D. 4',6-Diamidino-2-phenylindole, a fluorescent probe for tubulin and microtubules. *J. Biol. Chem.* **1985**, *260*, 2819−2825.

25. Diaz, J. F.; Andreu, J. M. Assembly of purified GDP-tubulin into microtubules induced by taxol and taxotere: reversibility, ligand stoichiometry, and competition. *Biochemistry* **1993**, *32*, 2747−2755.

26. Sinha, K.; Das., J.; Pal, P. B.; Sil, P. C. Oxidative stress: the mitochondria-dependent and mitochondria-independent pathways of apoptosis. *Arch. Toxicol.* **2013**, *87*, 1157−1180.

27. Afshari, C. A.; Barrett., J. C. Cell cycle controls: potential targets for chemical carcinogens? *Environ. Health Perspect.* **1993**, *101*, 9–14.

28. Jackman, M.; Lindon, C.; Nigg, E. A.; Pines, J. Active cyclin B1-Cdk1 first appears on centrosomes in prophase. *Nat. Cell Biol.* **2003**, *5*, 143–148.

29. Mollinedo, F.; Gajate., C. Microtubules, microtubule-interfering agents and apoptosis. *Apoptosis.* **2003**, *5*, 413–450.

30. Poruchynsky, M. S.; Wang, E. E.; Rudin, C. M.; Blagosklonny, M. V.; Fojo, T. Bcl-xl is phosphorylated in malignant cells following microtubule disruption. *Cancer Res.* **1998**, *58*, 3331–3338.

31. Haldar, S.; Basu, A.; Croce, C. M.; Bcl2 is the guardian of microtubule integrity. *Cancer Res.* **1997**, *57*, 229–233.

32. (a) Aprile, S.; Grosso, E. D.; Tron, G. C.; Grosa, G. In vitro metabolism study of combretastatin A-4 in rat and human liver microsomes. *Drug Metab. Dispos.* **2007,** *35*, 2252-2261. (b) Soussi, M. A.; Aprile, S.; Messaoudi, S.; Provot, O.; Grosso, E. D.; Bignon, J.; Dubois, J.; Brion, J. D.; Grosa, G.; Alami, M. The metabolic fate of *iso*combretastatin A-4 in human liver microsomes: identification, synthesis and biological evaluation of metabolites. *ChemMedChem* **2011,** *6*, 1781-1788.

33. Alami, M.; Brion, J. D.; Provot, O.; Peyrat, J. F.; Messaoudi, S.; Hamze, A.; Giraud, A.; Bignon, J.; Bakala, J.; Liu, J. M. *Iso*CA-4 and analogues thereof as potent cytotoxic agents inhibiting tubulin polymerization. Patent WO 122620 A1, 2008.

34. Bi, H. C.; Zuo, Z.; Chen, X.; Xu, C. S.; Wen, Y. Y.; Sun, H. Y.; Zhao, L. Z.; Pan, Y.; Deng, Y.; Liu, P. Q.; Gu, L. Q.; Huang, Z. Y.; Zhou, S. F.; Huang, M. Preclinical

factors affecting the pharmacokinetic behaviour of tanshinone IIA, an investigational new drug isolated from Salvia miltiorrhiza for the treatment of ischaemic heart diseases. *Xenobiotica* **2008**, *38*, 185–222.

35. Bradford, M. M. A rapid and sensitive method for the quantitation of microgram quantities of protein utilizing the principle of protein-dye binding. *Anal. Biochem.* **1976**, *72*, 248–254.

Table of contents graphic: